Identification of Core Yeast Species and Microbe-Microbe Interactions Impacting Larval Growth of *Drosophila* in the Wild

Authors

Ayumi Mure[1], Yuki Sugiura[2], Rae Maeda[2], Kohei Honda[1], Nozomu Sakurai[3], Yuuki Takahashi[1], Masayoshi Watada[4], Toshihiko Katoh[1], Aina Gotoh[1], Yasuhiro Gotoh[5], Itsuki Taniguchi[5], Keiji Nakamura[5], Tetsuya Hayashi[5], Takane Katayama[1], Tadashi Uemura[1,6,7], and Yukako Hattori[1,8*]

Affiliations

[1] Graduate School of Biostudies, Kyoto University, Kyoto, Japan

[2] Center for Cancer Immunotherapy and Immunobiology, Kyoto University, Kyoto, Japan

[3] National Institute of Genetics, Mishima, Japan

[4] Graduate School of Science and Engineering., Ehime University, Matsuyama, Japan.

[5] Graduate School of Medical Sciences, Kyushu University, Fukuoka, Japan

[6] Center for Living Systems Information Science, Kyoto University, Kyoto, Japan

[7] AMED-CREST, Tokyo, Japan.

[8] JST FOREST, Tokyo, Japan.

[*] Correspondence: yhattori@lif.kyoto-u.ac.jp (Y.H.)

ABSTRACT

Microbiota consisting of various fungi and bacteria have a significant impact on the physiological functions of the host. However, it is unclear which species are essential to this impact and how they affect the host. This study analyzed and isolated microbes from natural food sources of *Drosophila* larvae, and investigated their functions. *Hanseniaspora uvarum* is the predominant yeast responsible for larval growth in the earlier stage of fermentation. As fermentation progresses, *Acetobacter orientalis* emerges as the key bacterium responsible for larval growth, although yeasts and lactic acid bacteria must coexist along with the bacterium to stabilize this host-bacterial association. By providing nutrients to the larvae in an accessible form, the microbiota contributes to the upregulation of various genes that function in larval cell growth and metabolism. Thus, this study elucidates the core microbial species that support animal growth under microbial transition.

INTRODUCTION

In nature, animals live in association with a diverse community of microorganisms. These associated microbes, especially fungi and bacteria, perform a range of beneficial functions for their host, such as nutrient provision and immune modulation (Ikeda-Ohtsubo et al., 2018; Zheng et al., 2020). Some of these host-microbe associations are facultative and dispensable, while others are more important or even essential for host growth or survival under specific circumstances. Compared to symbioses between a limited number of specific species (Shigenobu & Wilson, 2011; Su et al., 2022), however, those that encompass a larger number of species are intricate and analytically challenging. Additionally, despite a growing number of reports documenting the presence of fungi in the mammalian intestine, including humans, our comprehension of their roles is still limited, with the exception of a handful of pathogenic fungi (Hallen-Adams & Suhr, 2017; Pérez, 2021). Moreover, the composition of these complex microbiota tends to change over time (Moya & Ferrer, 2016; Qiu et al., 2021). Therefore, we focused on how the host sustains its life processes in such unstable environments.

Drosophila melanogaster has made remarkable contributions to our comprehension of the regulatory mechanisms governing development, growth, and metabolism, which are highly conserved among animals. More recently, the fly has emerged as a valuable model for investigating animal-associated microbes. The microbiota associated with *Drosophila* comprise relatively few species, most of which can be cultured aerobically (Chandler et al., 2011, 2012; Grenier & Leulier, 2020; Lee & Brey, 2013). Furthermore, germ-free or gnotobiotic animals can be easily prepared (Ludington & Ja, 2020). The aforementioned advantages of analysis enabled a thorough exploration of the role of *Drosophila*-associated microbes. Notably, lactic acid bacteria (LAB) and acetic acid bacteria (AAB) demonstrate the ability to enhance larval growth under nutrient scarcity (Shin et al., 2011; Storelli et al., 2011). However, most researchers have examined only a single species or a limited number of bacteria. Additionally, most previous studies did not investigate the association with yeasts. Possibly, this is because live yeasts are either absent or present in very small quantities, due to antifungal agents added to the *Drosophila* laboratory foods. Instead of live yeasts, the foods typically contain heat-killed budding yeast *Saccharomyces cerevisiae* as a major nutrient source, but this yeast species rarely coexists with *Drosophila* in the wild (Hoang et al., 2015). Consequently, the relationship between *Drosophila* and its associated microorganisms has often been classified as facultative (Gallo et al., 2022; Martino et al., 2018), and the role played by associated fungi has been largely overlooked.

In the wild, the presence of microbes is crucial for the developmental growth of *Drosophila* larvae that feed on fruit-based food sources. *D. melanogaster* in its natural habitat feeds on fruits fermented by its associated microbes (Watanabe et al., 2019). Germ-free larvae cannot grow on fresh fruits alone, while inoculation with certain species of yeasts or bacteria promotes pupariation (Anagnostou et al., 2010; Pais et al., 2018). These findings suggest that, in the wild, microbes provide vital nutrients for larval growth. While the bacterial roles have been extensively investigated, few reports have focused on yeasts; some studies described interspecies variation of yeasts with regard to their effects on larval growth (Anagnostou et al., 2010; Quan & Eisen, 2018; Solomon et al., 2019), but the underlying mechanisms have not been thoroughly explored. We therefore set out to address the following questions: (1) which species play a central role in food microbiota? (2) what are the essential traits that these species possess? (3) what microbe-derived nutrients are necessary for host growth?

To address these questions, we sampled fermented bananas that had been fed upon by wild *Drosophila* species. We collected the foods at two different timepoints, referred to as "early-stage" and "late-stage" foods, and demonstrated a dramatic shift in fungal and bacterial taxonomic compositions during fermentation. Regarding fungi, we observed that yeasts predominated in both stages, but the dominant species changed between the stages. Among bacterial species, Enterobacteriales accounted for a large proportion in the early stage, whereas LAB and AAB dominated in the late stage. We then isolated yeast and bacterial strains from the food samples and tested their ability to support larval development on a banana agar. *Hanseniaspora uvarum*, the predominant yeast species in the early stage, was able to support larval growth by itself. In contrast, most of the late-stage microbes tested did not efficiently promote larval growth when inoculated individually. However, we found that when the acetic acid bacteria *Acetobacter orientalis* coexisted with either LAB or late-stage yeast species, it effectively promoted larval growth. Our analyses of larvae under different microbial environments, including transcriptomic analyses of first-instars, strongly suggest that *A. orientalis* is potentially able to promote larval growth, although it requires interactions with other late-stage microbes. Finally, we investigated the molecular basis underlying the distinct larval growth-promoting effects among yeast species, including the supportive *H. uvarum* from the early-stage foods and non-supportive *Pichia kluyveri* and *Starmerella bacillaris* from the late-stage foods. Surprisingly, all the yeast species strongly promoted larval growth upon heat killing. This and additional results indicate that all species produce sufficient nutrients for larval development, but larvae cannot utilize those produced by the live non-supportive species. Our metabolomic analysis and metabolite supplementation assay suggest that only the supportive yeast cells can release critical metabolites for larval growth, including branched-chain amino acids, leucine and/or isoleucine. Collectively, our findings detail the core microbial species, their interactions, and the yeast species-dependent supply of nutrients that contribute to the development of *Drosophila* larvae in nature.

RESULTS

The composition of both yeast and bacteria in the food microbiota shifts as fermentation progresses, independently of the presence of larvae

To examine the community structure of the microbiota associated with *Drosophila* larvae in nature, we collected and analyzed fermented foods that had been fed on by wild larvae (Figure 1A, Table S1A). Because *D. melanogaster* and its related species are often found near human settlements, we set traps containing freshly peeled and sliced bananas outside of our residences so that wild flies would lay eggs on the foods. A portion of each fermented food sample was collected as "early-stage" food, while the remaining food was incubated in the laboratory. When the larvae reached the late third-instar stage, we collected further fermented "late-stage" food samples (refer to MATERIALS AND METHODS for experimental definitions of early- or late-stage foods). We performed sequencing of the fungal internal transcribed spacer (ITS) region and the bacterial 16S rRNA region to analyze the composition of fungi and bacteria in individual samples, respectively (Figure 1B; Tables S2A and S2B).

In most samples, yeasts consistently accounted for a major proportion of the fungal communities (top of Figure 1B; Table S2A), as previously reported (Chandler et al., 2012). At the family level, the compositions showed dramatic differences between the early and late stages; while Saccharomycodaceae dominated in most of the early-stage foods, Pichiaceae, *Starmerella*, and Saccharomycetaceae became dominant in the late-stage foods. The dominant bacteria also differed between the two stages, with Enterobacteriales predominating at the early stage and lactic acid bacteria (LAB) and acetic acid bacteria (AAB) predominating at the late stage (bottom of Figure 1B; Table S2B). Henceforth, we refer to the transition from early-to-late stages in microbial composition as the microbial composition shift or simply the composition shift. In this sampling, we obtained, by chance, a “no-fly” trap; no adult flies were caught in the trap, and no eggs, larvae, or pupae were found in the food at either stage (“No-fly” in Figure 1B; “No-fly trap” in Tables S2A and S2B; refer to “Collection of fermented foods and wild *Drosophila* samples” section in MATERIALS AND METHODS for further details). We analyzed food samples from this trap for comparison. The microbiota in the foods significantly differed from that of other samples, with a lower percentage of yeast in the fungal community and a consistently high abundance of Enterobacteriales in the bacterial community.

A previous study showed that the presence of larvae influences the community structures of food microbiota (Stamps et al., 2012). Therefore, we sought to determine whether the larvae contributed to the composition shift (Figure 1C; Table S1B). We prepared microbe-containing suspensions using newly collected early-stage foods and introduced them to fresh bananas, with or without germ-free embryos. We then incubated the samples and examined whether the microbial composition shifts occurred in the bananas. Remarkably, the composition shifts occurred similarly, irrespective of the presence of larvae, as indicated by the decreased proportions of Saccharomycodaceae yeast and Enterobacteriales bacteria, along with the increased proportions of Pichiaceae yeast as well as LAB and AAB (compare “Susp” with “w/o L” or “w/L” in Figure 1D; see also Tables S2C and S2D). These findings suggest that the composition shift observed in the food microbiota is unlikely to be solely attributed to the presence of larvae but more plausibly influenced by factors such as interspecies interactions among microbes.

Furthermore, we analyzed the microbial composition of adult flies captured in traps, as well as the food and larval samples (Figure 1E; Table S1C). This analysis revealed a similar

composition of the yeast species in adult flies and early-stage foods, and a similar composition of yeast species in larvae and late-stage foods (top of Figure 1F; Table S2C). However, notable dissimilarities were observed in the bacterial compositions between the *Drosophila* samples and the early-stage foods, primarily attributed to the conspicuous presence of *Wolbachia* sp. (Anaplasmataceae) and *Gilliamella apicola* (Orbaceae) in the *Drosophila* samples (bottom of Figure 1F; Table S2E). Anaplasmataceae and Orbaceae are intracellular and gastrointestinal symbionts of insects, respectively (Kwong & Moran, 2013; Werren et al., 1995), which plausibly accounts for their relatively lower abundance in the food samples.

In addition to the community structures, we investigated whether there were alterations in the overall abundance of yeasts and bacteria between the early- and the late-stage foods. For this purpose, we performed quantitative RT-PCR to quantify the copy numbers of fungal and bacterial rDNA in each food sample presented in Figures 1B, 1D, and 1F (Figure S1). The analysis indicated that there were no dramatic increases or decreases in copy numbers in most food samples. Note that measuring rDNA copy numbers in the microbiome does not necessarily reflect actual cell numbers due to variations in the genomic rDNA copy numbers among species (Lofgren et al., 2019; Stoddard et al., 2015). Nonetheless, these results suggest that the quantities of microbes did not undergo substantial changes between the two stages.

Prominent acceleration of larval development is observed with early-stage-dominant yeast alone, as well as in combination with late-stage-dominant acetic acid bacteria and other microbes

As described in the previous section, we documented the presence of various yeast and bacterial species in fermented larval foods, the populations of which underwent notable compositional shifts over time. Previous studies suggest that different yeast or bacterial species contribute to larval development to varying degrees (Anagnostou et al., 2010; Consuegra, Grenier, Baa-Puyoulet, et al., 2020; Pais et al., 2018; Quan & Eisen, 2018; Solomon et al., 2019). Continuing this line of investigation, we undertook to identify which of the dominating microbial species in the early- or late-stage foods, either individually or as mixtures, promote larval development. To this end, we isolated fungal and bacterial strains from the food samples (refer to Table S3 and the "Isolation and species identification of microbes" section in MATERIALS AND METHODS for further details). We subsequently inoculated the isolated strains, either individually or in combinations, into a sterile banana-based food (banana agar), and introduced germ-free larvae. Thereafter, we evaluated the effects of the microbial species on the percentage and the timing of pupariation (see details in "Quantification of larval development" in MATERIALS AND METHODS). Note that on this food, larval development critically depends on associated microbes, as the larvae failed to pupariate on banana agar without microbes ("germ-free (GF)" in Figure 2A and subsequent figures).

To assess the impact of microbes found in early-stage foods on larval development, we employed yeast strains belonging to *Hanseniaspora uvarum*, which dominated in the early-stage foods, or *Pichia kluyveri*, which was also detected in the foods (Table S2A; also represented by the darkest and the second darkest brown bars in the top of Figure 1B), along with a bacterial strain of *Pantoea agglomerans*, which constituted the sole dominant bacterial genus (Table S2B; also represented by cyan bars at the bottom of Figure 1B). We investigated whether each strain or a combination of the strains promotes larval development (Figures 2A, 2B, S2A, and S2B). When

inoculated individually, *H. uvarum* and *Pa. agglomerans* effectively promoted larval growth ("Y_2" and "E" in Figures 2A and 2B, respectively; "Y_1" and "E" in Figures S2A and S2B, respectively; see also Table 1), whereas *Pi. kluyveri*, another yeast species, had almost no promoting effect ("Y_1" in Figures 2A and 2B; "Y_2" in Figures S2A and S2B). When the strains were combined, we observed a significantly accelerated larval development in the presence of *H. uvarum* ("1: Y_1Y_2" and "3: Y_1Y_2E" in Figures 2A and 2B) than in its absence ("2: Y_1E" in Figures 2A and 2B). Hence, in the early-stage foods, *H. uvarum* played a critical role in promoting larval development.

A similar feeding experiment was conducted using a total of five stocks of the late-stage microbes (Figures 2C, 2D S2C, and S2D; Table 1): two dominating late-stage yeast species, the most predominant LAB and AAB species (Table S2B; see also green and orange in the bottom of Figure 1B, respectively), and *Pa. agglomerans*, which persisted from the early stage, albeit in a smaller proportion (Table 1). When fed individually, none of the yeast or bacterial species efficiently supported larval growth, except for *Pa. agglomerans* (lines and symbols with different brightness of gray in Figure 2C). Conversely, when larvae were fed mixtures, their development was almost equally efficient as long as LAB and AAB coexisted (color-coded in blues in Figure 2C). In this experiment, the coexistence effects of yeast and acetic acid bacteria were not tested. Therefore, we repeated the experiment using only one strain from each of the most dominant yeast, LAB, and AAB species (see the tables in Figures 2F and S2F). Larval development, in terms of both the pupariation rate and timing, was promoted when the AAB *A. orientalis* was inoculated together with either a yeast (*Starmerella bacillaris* or *Pi. kluyveri*) or a LAB (*Leuconostoc mesenteroides* or *Lactiplantibacillus plantarum*) (Figures 2E, 2F, S2E and S2F). This result suggests that, in the late-stage foods, the coexistence of AAB and other microbial species, yeasts or LAB, was critical for larval development. Additionally, we investigated the eclosion of pupae under different microbial conditions and confirmed that a majority of the pupae successfully eclosed, albeit with some variation observed across experiments (Figure S3).

To summarize these results, strong promotion of larval development was observed when the larvae were associated with an early-stage yeast *H. uvarum*, or a combination of *A. orientalis* and other late-stage microbes.

During the late stage, acetic acid bacteria play a crucial role in supporting larval development through interspecies interactions among the microbes

To investigate how larvae respond to the different microbial conditions, we conducted whole-body RNA-seq of gnotobiotic first-instar larvae that were subjected to a 15-hour feeding period on banana agar (Table S4). The agar was either kept sterile or inoculated with yeast *H. uvarum*, LAB, or AAB individually, or a combination of LAB and AAB (Figure 3A-D). Remarkably distinct gene expression profiles were observed between the "supportive" conditions, where larvae efficiently pupariated in the previous experiments ("Yeast" and "LAB+AAB" in Figure 3A), and the "non-supportive" conditions, where larval development was markedly impaired ("LAB" and "GF" in Figure 3A). Notably, a multitude of genes involved in metabolism and cell growth displayed significant upregulation in response to the AAB and LAB mixtures when compared to LAB alone (Figures 3B, 3C, S4A, and S4B). Moreover, differentially expressed genes under the supportive and the non-supportive conditions exhibited strikingly similar profiles to those reported in a previous investigation of fed and starved conditions (Zinke et al., 2002; Figure 3D).

Interestingly, although larvae fed on AAB alone largely failed to pupariate ("A" in Figures 2C-2F), their gene expression profile after the 15-hr feeding period closely resembled that of the supportive conditions (compare "AAB" with "Yeast" and "LAB+AAB" in Figure 3A). This result implies that AAB possessed the ability to induce a growth-promoting response, but the effect likely did not persist until pupariation. We observed that the growth rate of AAB on banana agar was notably lower compared to those of other microbes. This led us to speculate that this lower growth rate might result in a shortage of AAB, leading to undernutrition during the later stage of larval development. To test this hypothesis, we investigated whether larval development could recover when AAB was constantly available. Daily supplementation of AAB enabled larvae to pupariate as effectively as the initial co-inoculation of AAB and LAB did (Figures 3E and 3F), demonstrating that AAB can promote larval growth if it is available throughout the course of development.

The aforementioned observations have prompted us to assume that yeast and LAB contribute to the stable coexistence of AAB and larvae. To investigate this hypothesis, we raised larvae on a diet containing AAB either alone or in conjunction with the other species. After a 4-day incubation, we quantified the abundance of AAB in each tube, including those in the food and those inside the larval body. In most of the combinations, co-inoculation with other species led to a 5-19 fold increase in the number of AAB colonies compared to the monoculture conditions (Figures 3G and 3H). These findings suggest that AAB plays a crucial role in providing nutrients during the late stages of larval development, while other microbial species support a stable association between AAB and larvae.

Thus, none of AAB, LAB, or the yeast in the late-stage foods strongly promoted larval growth individually, while mixing AAB with LAB or the yeasts did (Figures 2C-2F and S2C-S2F). All of our results so far strongly suggest that these interspecies interactions among the microbes underlie the promotion of larval growth by late-stage microbiota.

The isolated yeast species promote varying degrees of larval development, but all support larval development upon heat killing

We found that the early-stage yeast *H. uvarum* facilitated larval development, whereas the dominant yeasts in the late stage, *Pi. kluyveri* and *St. bacillaris*, did not (Figure 2A-2D and S2A-S2D). To elucidate the underlying mechanisms behind these diverse outcomes, we conducted comprehensive comparative analyses with the respective yeasts. We used six yeast species that originated from the fermented foods (*Kazachstania humilis*, *Martiniozyma asiatica*, and *Saccharomycopsis crataegensis* in addition to the aforementioned three species) and a laboratory strain of the model species *Saccharomyces cerevisiae*, which was not detected in our food samples (Figure 4).

When we provided each species to germ-free larvae, the larvae fed on *H. uvarum* showed the highest percentage of pupariation, while larvae fed on *K. humilis* or *M. asiatica* also pupariated at relatively high rates, albeit with a slower timing for *M. asiatica* (Figures 4A and 4B). We classified these three species as the "supportive" yeast species. In contrast, larvae fed on *Pi. kluyveri* or *St. bacillaris*, which are the dominant species during the late stage, showed notably low percentage of pupariation, leading to their classification as "non-supportive" (Figures 4A and 4B). Inoculation with *Saccharomycopsis crataegensis* or an laboratory strain of *Saccharomyces cerevisiae* BY4741 resulted in reduced percentages and delayed timing of pupariation compared to the inoculation

with supportive species, thus earning the designation of "mild." These results underscore the variable abilities of individual yeast species to promote larval development.

To investigate the response of larvae to different yeast species, we conducted whole-body RNA-seq analysis of larvae (Table S5). The overall findings closely resembled those obtained from various bacterial species (Figures 4C-4F, S4C, and S4D; cf. Figures 3A-3D, S4A, and S4B). Gene expression profiles exhibited marked differences between larvae fed on the supportive yeasts and those fed on the non-supportive yeasts, with intermediate responses observed in larvae fed on the mild yeasts (Figure 4C). Feeding on the supportive yeasts upregulated genes involved in metabolism and cell growth (Figures 4D and 4E), and the expression profiles under the supportive and the non-supportive yeast diets resembled those observed in fed and starved conditions, respectively (Figure 4F).

One potential factor determining the ability of larvae to develop on specific yeast species might be the production or secretion of adequate nutrients for larval growth. To assess whether each yeast species produced sufficient essential nutrients internally, we administered heat-killed yeasts to the larvae. Somewhat surprisingly, strong growth enhancement was observed in all seven yeast species upon heat killing, with *Pi. kluyveri* and *St. bacillaris* promoting larval development nearly as effectively as the supportive yeasts (Figures 4G and 4H). We further explored the effect of killing the yeasts using banana agar supplemented with antifungal agents (10 mL/L 10% p-hydroxy-benzoic acid in 70% ethanol and 6 mL/L propionic acid, following the concentration described in Kanaoka et al., 2023), and observed similar growth promotion by *Pi. kluyveri* and *St. bacillaris* (data not shown). This finding suggests that all of these yeasts do indeed produce the requisite nutrients for larval development; however, it is likely that the nutrients produced by the live non-supportive yeasts are inaccessible to larvae (further analyzed in the subsequent section).

We also considered the possibility that the non-supportive yeasts somehow inhibited the host growth. To test this possibility, we cultured the yeast species on a nutrient-rich sterile medium and fed them to the larvae (Figure 4I and 4J). This medium contains dry yeast and enables larvae to pupariate even without live yeasts ("GF" in Figure 4I and 4J). Under these conditions, larvae fed with *St. bacillaris* pupariated as efficiently and nearly as rapidly as those without yeasts or with other yeast species, suggesting that *St. bacillaris* did not impede larval growth (Figures 4I and 4J). In contrast, larvae fed with *Pi. kluyveri* exhibited a significantly reduced percentage of pupariation compared to larvae grown with the other yeast species or without yeasts. This could be related to the extensive growth of *Pi. kluyveri* on this food (Figure S4E). Nevertheless, none of these yeast species reproduced the low percentage of pupariation of larvae observed on banana agar. Therefore, the inhibitory effects of *Pi. kluyveri* and *St. bacillaris* are less likely.

Supportive yeasts facilitate larval growth by producing nutrients, including branched-chain amino acids, and releasing them from their cells

Given that the non-supportive yeast species supported larval growth upon heat-killing, we hypothesized that the key distinction between the supportive and the non-supportive species lies in their ability to release nutrients contained within the cells. To test this hypothesis, we conducted a metabolomic analysis of the two supportive species (*H. uvarum* and *K. humilis*) and the two non-supportive species (*Pi. kluyveri* and *St. bacillaris*) and analyzed not only the yeast cells but also

320 two additional samples anticipated to contain metabolites released from the cells: yeast-
321 conditioned banana-agar plates and cell suspension supernatants. (Figure 5A-5F, Table S6).

322 In the yeast-conditioned banana-agar plates, which were anticipated to contain yeast-derived
323 nutrients, many well-known nutrients included in a chemically defined synthetic (holidic) medium
324 for *Drosophila melanogaster* (Piper et al., 2014, 2017) were not increased compared to the sterile
325 banana-agar plates; instead, they exhibited drastic decreases irrespective of the yeast species
326 (Figures 5A and 5B). The quantities of metabolites within the cells varied markedly among the
327 species (Figures 5C and 5D); while the supportive *H. uvarum* contained numerous known
328 metabolites, it was intriguing that *K. humilis*, another supportive species, did not possess as many
329 essential nutrients as other species, including the non-supportive *Pi. kluyveri* and *St. bacillaris*
330 (Figure 5D). This result, in conjunction with the observations from feeding heat-killed yeasts
331 (Figure 4G and 4H), raises the possibility that the interspecies disparities in metabolites within
332 living yeast cells do not directly influence larval growth. On the other hand, our analysis of the
333 cell suspension supernatant revealed distinct variations in the known nutrients in the holidic
334 medium between the supportive and non-supportive species (Figures 5E and 5F). Among these,
335 we focused on branched-chain amino acids (BCAAs), leucine and isoleucine (Figure 5F). Previous
336 studies have demonstrated that bacteria associated with *Drosophila* provide these essential amino
337 acids to the hosts feeding on artificial diets lacking them (Consuegra, Grenier, Akherraz, et al.,
338 2020; Henriques et al., 2020; B. Kim et al., 2021). In our analysis, suspension supernatants of
339 supportive yeasts had concentrations of both leucine and isoleucine that were at least four-fold
340 higher than those of non-supportive yeasts (Figures 5F-5H; see also Table S6B).

341 The above finding prompted us to explore whether leucine and isoleucine are supplied by the
342 associated supportive yeasts, similar to bacterial symbiosis. To investigate this, we supplemented
343 banana agar with these BCAAs and inoculated it with the non-supportive yeasts, subsequently
344 evaluating the restoration of larval development (Figures 6A and 6B). Remarkably, the
345 supplementation of BCAAs elicited a significant improvement in larval development in the
346 presence of the non-supportive yeasts, while it had no effect on larvae fed with the supportive
347 yeasts (Figures 6A and 6B). At 12 days after egg laying, a significant increase was observed in the
348 proportion of individuals that had progressed to the second instar or later stages (Figure 6B). These
349 results suggest that the lack of BCAAs in bananas inoculated with the non-supportive yeast species
350 is one of the causes of larval growth deficiency. Additionally, we explored the conservation of the
351 biosynthetic pathways responsible for leucine and isoleucine among the isolated yeast strains. We
352 performed *de novo* genome assembly and annotation for the six yeast species and examined the
353 presence of orthologs (Table S7). This analysis, along with a subsequent RNA-seq analysis of the
354 yeast species, revealed the conservation of the biosynthetic pathways of these amino acids across
355 all the isolated yeasts (Figure 6C; Table S8). The result of this genomic analysis also strengthens
356 the possibility that differences in the ability of yeasts to support larvae do not stem from variances
357 in their ability to biosynthesize BCAAs, but rather in their ability to provide BCAAs in an available
358 form to the larvae.

359 We noted, however, that the supplementation of BCAAs alone did not completely restore the
360 growth of larvae that fed on the non-supportive yeasts. Despite attempts to enhance growth by
361 increasing the BCAA concentration five- or ten-fold, no improvement was observed (data not
362 shown). We also supplemented the banana agar with other metabolites, including nicotinic acid
363 and/or lysine and asparagine, which were detected in higher amounts within the suspension
364 supernatants of the supportive yeasts, individually or in combination with the BCAAs. None of

these additions had any effect on larval growth (data not shown). These results suggest that other crucial nutrients are provided by the supportive yeasts.

Regarding the mechanism of nutrient release, one possibility is their secretion from live cells, while another possibility is their leakage from dead cells. To address the latter hypothesis, we collected cells of the four yeast species from banana-agar plates and stained dead cells using Phloxine B (Figures 6D-6G). Noticeably more dead cells were found in the supportive *K. humilis* compared to other species (Figure 6E), implying that nutrients leak from dead *K. humilis* cells into the food, which is subsequently utilized by the larvae.

DISCUSSION

In this study, we have shown that the composition of the microbiota shifts dramatically as fermentation progresses. Each individual microbial species plays a crucial and indispensable role in promoting host growth, either through the provision of essential nutrients or by establishing a stable association between the host and the nutrient-providing species (Figure 6H). The capacity of yeasts to facilitate larval growth seems to rely on their ability to extracellularly release essential nutrients, such as leucine and/or isoleucine, thereby making these nutrients accessible to the host. These microbial functions have effectively empowered the host to grow on a nutritionally inadequate fruit.

Drosophila has been known to co-exist with yeast and bacteria in nature (Chandler et al., 2011, 2012; Corby-Harris et al., 2007; Cox & Gilmore, 2007; Quan & Eisen, 2018; Shihata & Mrak, 1952). Our investigation reveals substantial shifts in both fungal and bacterial compositions during fermentation, which coincides with alterations in the species serving as nutrient sources. A previous study reported that *Drosophila* larvae have profound effects on the community structure of yeasts in fermented bananas (Stamps et al., 2012). Our experiment, however, suggests that the microbial composition shift observed in our food samples is unlikely to be solely attributed to the presence of larvae but is more plausibly influenced by factors such as interspecies interactions among microbes. These discrepancies may be due in part to differences in experimental conditions such as larval densities, food sample volumes, or culture vessels. The initial microbial inoculation to foods is assumed to be mediated by adult flies (Broderick & Lemaitre, 2012). Our results imply that the inoculation leads to the dominance of *H. uvarum*, which can support larval growth on its own. Consequently, a microbially self-regulated transition occurred, leading to the dominance of microbial communities, including AAB, LAB, and the late-stage yeasts.

In the early stage of fermentation, both the predominant yeast and bacterial species were capable of supporting larval growth on their own. However, in stark contrast, at the late stage of fermentation, microbial interactions assumed a crucial role. While AAB provide sufficient nutritional resources to support larval growth, their growth rate on bananas is suboptimal. On the other hand, other associated microbes may lack essential nutrients for larvae but contribute to establishing a stable association between AAB and the larvae. Previous studies have reported interactions between AAB and LAB in artificial foods, where AAB act as a source of nutrients, including amino acids, while LAB provide lactic acid as a substrate for amino acid biosynthesis (Consuegra, Grenier, Akherraz, et al., 2020; Henriques et al., 2020). Our findings have demonstrated that LAB also play a supportive role in the symbiotic relationship between larvae and AAB on a fruit, a natural food source of *Drosophila* larvae. It is worth noting that interactions may also occur between the AAB and the late-stage yeasts. We observed the presence of various metabolites not only in the suspension supernatant of the supportive yeast species but also in that of the non-supportive late-stage yeast species. Therefore, the growth of AAB on fruits could be enhanced through the utilization of such metabolites by the bacterium.

In laboratory settings, yeasts are recognized and employed as important nutritional sources for *Drosophila*, providing essential nutrients such as amino acids, vitamins, and fatty acids (Baumberger, 1917; Broderick & Lemaitre, 2012). In our study, we have demonstrated that during larval growth on their natural food sources, the associated yeasts contribute to the provision of BCAAs, leucine and/or isoleucine. Of these two amino acids, the availability of leucine acts as an effective regulatory signal for the mTORC1 pathway, as established in both mammals and *Drosophila* (Fox et al., 1998; Gu et al., 2022; J. Kim & Guan, 2019; Zhang et al., 2021). The

mTORC1 pathway governs metabolism and cell growth in response to nutritional conditions. Indeed, the expression levels of numerous genes involved in these processes exhibited significant up- or down-regulation in larvae fed on supportive microbes compared to those fed on non-supportive microbes or germ-free individuals. Nonetheless, supplementing these branched-chain amino acids (BCAAs) alone did not fully restore larval growth, suggesting that there should be other key nutrients. Our metabolomic analysis did not encompass some known metabolites, including lipids. Among these, sterols, substrates for ecdysone biosynthesis, are indispensable for larval growth. However, sterols are unlikely to be lacking in the fermented bananas. In our experiments, *Pa. agglomerans* and *A. orientalis* did promote larval growth, but most bacteria, including the two aforementioned species, lack the steroid biosynthesis pathway (Hoshino & Gaucher, 2021). Therefore, larvae can grow on bananas without bacterial-derived sterols. Deficiency in other lipids is also unlikely, because larvae can grow on the holidic medium for *D. melanogaster* that contains cholesterol as a sole lipid component, and the developmental delay on the medium is rescued by a "critical element" which is "not a lipid" (Piper et al., 2014). Therefore, microbial nutrients that promote larval growth, whose functions have not yet been identified in this study, may be components other than lipids.

Despite the well-recognized importance of yeast as a source of nutrients, limited studies have reported the detailed process of how these nutrients are utilized by larvae. Our results suggest that for yeasts to serve as nutritional sources, they should not only produce the nutrients, but also release them outside the cells. The amount of nutrients released extracellularly varied among yeast species, which could be explained by varying abilities to secrete metabolites. Another possibility suggested for *K. humilis* was that this species is more prone to death on the culture medium, thus releasing more nutrients. Our metabolomic analysis of yeast-conditioned culture medium also suggested that the released nutrients do not accumulate in the medium but are likely to be eventually taken up and utilized by the yeast themselves. Further investigation is required to elucidate the nutritional dependence and competition between yeast and larvae.

Our results indicate that yeast cells are not necessarily digested in the larval gut, which might contradict previous reports. For instance, vegetative cells of *Saccharomyces cerevisiae* have been reported to be digested in the gut of adult flies (Coluccio et al., 2008). However, the digestibility of yeast may vary depending on the species of yeast, diet composition, or developmental stage of the host. Indeed, a study has discussed the possibility that *St. bacillaris* is not digested in the larval gut (Solomon et al., 2019). In our study, by focusing on the non-model yeast species associated with wild flies, we revealed part of the mechanism by which wild *Drosophila* larvae utilize yeast as a nutrient source.

To date, the majority of studies on animal-associated yeasts have focused on a limited number of specific species that are either pathogenic or employed for fermenting foods. In this study, we have examined the species composition of yeasts that make up the symbiotic mycobiota of *Drosophila* and analyzed the roles of each predominant species by investigating their interactions with bacteria as well as with the host. To obtain a comprehensive and detailed understanding of the function of animal microbiota, future studies should further explore the contribution of associated yeasts.

461 **MATERIALS AND METHODS**

462 ***Drosophila melanogaster* strains and culture**

463 *D. melanogaster Canton-Special* (E-10002) strain was obtained from EHIME-Fly *Drosophila*
464 Stocks of Ehime University. This strain was used for all the experiments unless otherwise noted.
465 *Cg-GAL4* was a gift from H. Asha (Asha et al., 2003). The stocks were reared on a laboratory
466 standard diet as previously described (Watanabe et al., 2017).

467 Yeast-based nutrient-rich diet was prepared following the instructions at Bloomington Stock
468 Center (https://bdsc.indiana.edu/information/recipes/germanfood.html). Reagents used are
469 described in Kanaoka et al., 2023. The preservatives (propionic acid and 10% p-hydroxy-benzoic
470 acid methyl ester) were omitted.

471

472 **Generation of germ-free larvae**

473 Germ-free animals were prepared as previously described (Watanabe et al., 2019) with minor
474 alterations. Briefly, embryos were collected on apple agar plates topped with yeast paste, and were
475 incubated at 25°C for 12-15 or 14.5-17.5 h. They were subsequently dechorionated in 50% bleach,
476 followed by washes with sterile water, 70% ethanol, and sterile water once more. The embryos
477 were placed on sterile agar plates and incubated at 25°C until newly hatched larvae were obtained.

478

479 **Collection of fermented foods and wild *Drosophila* samples**

480 Fermented food samples were collected using traps placed outdoors, near the authors' apartments
481 or houses in Kyoto and Osaka prefectures, Japan, or outside the laboratory at Kyoto University.
482 Within each trap made from an empty milk carton, ripening bananas, freshly peeled and cut into
483 small pieces, were placed in a sterile 100 mL centrifuge tube (Iwaki). 2.5 days later, wild flies
484 were found in all traps except for one (no-fly trap). The traps were collected, and 3-5 mL of the
485 foods (early-stage foods) were sampled. The remaining foods were incubated at 25°C, and 4-5
486 days later, when late 3rd instar larvae were seen in all foods except for the one from the no-fly trap,
487 the foods were collected (late-stage). At the first sampling, we added germ-free embryos of GFP-
488 expressing *D. melanogaster* laboratory strain (*Cg-Gal4, UAS-mCD8:GFP*) to obtain *D.*
489 *melanogaster* larvae that were reared in the fermented food, but we could not sample them because
490 most animals apparently drowned in the juice that seeped out of the fermented bananas.

491 To obtain early-stage-food suspensions, newly obtained early-stage foods were crushed in
492 PBS, and after vigorous mixing, the liquid was collected carefully without taking banana, embryos,
493 or larvae. 200 µL of this microbial suspension (or sterile PBS for Blank) was added to 100 mL
494 tubes containing fresh ripening banana with or without ~200 germ-free embryos (*Cg-Gal4, UAS-*
495 *mCD8:GFP*). The samples were incubated at 25°C for 4 days. Late-stage foods were collected as
496 described above. Larvae collected from the food were examined under a fluorescent microscope
497 to make sure they were derived from the embryos we added and not from contaminating wild
498 embryos. When sterile PBS was added to bananas instead of microbial suspensions in Figure 1C,
499 the food showed no apparent change in appearance or odor during the 4-day incubation, and larvae
500 in the food remained at the first instar stage. The amounts of microbes detected in such foods were

less than those obtained for the food inoculated with the microbial suspension by 2-4 orders of magnitude ("Blank" in Figure S1C and S1D; see details in the legend)."

All the food samples were collected after removing embryos and larvae, and snap-frozen. Larvae were surface-sterilized using the same procedure as embryo samples before snap-freezing. Adult flies in the traps were collected following different procedures depending on whether their microbiota were analyzed. When the samples were solely utilized for species identification, the whole bodies were stored in 100% or 70% ethanol. When we also required samples for microbial analysis, after washing the whole bodies in 70% ethanol, the head, external genitalia, and wings of each fly were removed and stored in 70% ethanol and subsequently used to identify the species. The rest of the body was snap-frozen and later used for the microbial composition analysis. Adult flies collected in each sampling are listed in Table S1.

All tools were sterilized prior to use. Frozen samples were stored at -80°C. Adult or larval samples collected from a single trap or food, respectively, were stored as a pool.

ITS or 16S rDNA sequencing analysis

Food, larval, or adult samples were freeze-dried for 2-3 days, followed by homogenization with 5 mm and 3 mm zirconium beads. Microbial DNA was extracted using a QIAamp DNA Stool Mini Kit (QIAGEN).

Library preparation, sequencing, and data analyses were performed by Macrogen Japan (Tokyo, Japan). For fungal analysis, the ITS region was amplified with primers ITS3 (5'-TCGTCGGCAGCGTCAGATGTGTATAAGAGACAGGCATCGATGAAGAACGCAGC-3') and ITS4 (5'-GTCTCGTGGGCTCGGAGATGTGTATAAGAGACAGTCCTCCGCTTATTGATATGC-3'). For bacterial analysis, the V3–V4 region of 16S rRNA was amplified with primers 341F (5'-TCGTCGGCAGCGTCAGATGTGTATAAGAGACAGCCTACGGGNGGCWGCAG-3') and 805R (5'-GTCTCGTGGGCTCGGAGATGTGTATAAGAGACAGGACTACHVGGGTATCTAATCC-3'). The amplicons were sequenced on an Illumina MiSeq sequencer (300 bp paired-end).

The paired-end reads were assembled using FLASH (Magoč & Salzberg, 2011), followed by pre-processing and clustering using CD-HIT-OTU (clustering cutoff = 99%). Taxonomy was assigned using QIIME (Caporaso et al., 2010) using the UNITE database (Nilsson et al., 2019) for fungal ITS, and the Ribosomal Database Project (RDP) database (Cole et al., 2014) for bacterial 16S rDNA (outputs can be found in Tables S2F-S2J), followed by manual correction and reassignment, in which reads originating from *Drosophila* spp. or banana (including chloroplast) were removed, and fungal and bacterial taxonomy was reassigned by NCBI BLAST search against the Nucleotide collection (nr/nt) database or using the RDP sequence match tool, respectively (Cole et al., 2014; Johnson et al., 2008). Sequences with the highest query cover and identity in blastn, or the highest S_ab score in RDP sequence match were considered as top hits. OTUs that had no top hits with an assigned species name or with top hits that belonged to more than one genus were marked as "Unassigned."

542 **qRT-PCR of ITS or 16S rDNA**

543 Quantification of fungal ITS or bacterial 16S rDNA was performed by quantitative real-time PCR
544 with THUNDERBIRD SYBR qPCR Mix (TOYOBO). DNA extracted from fermented food or
545 wild *Drosophila* spp. samples were diluted 10-100 fold before use. After an initial denaturation at
546 95°C for 1 min, 45 cycles of PCR were carried out: 95°C for 15 sec, 55°C for 30 sec, and 72°C for
547 50 sec. ITS or 16S rDNA amplicons derived from *Hanseniaspora uvarum* or *Pantoea agglomerans*,
548 respectively, were used for the generation of standard curves. The following primers were used:

549

550 For fungal ITS (White et al., 1990)

551 ITS3: 5'-GCATCGATGAAGAACGCAGC-3'

552 ITS4: 5'-TCCTCCGCTTATTGATATGC-3'

553 For bacterial 16S (Hugerth et al., 2014)

554 341F: 5'-CCTACGGGNGGCWGCAG-3'

555 805R: 5'-GACTACHVGGGTATCTAATCC-3'

556

557 Microbial rDNA copy numbers were calculated by multiplying the RT-PCR results by the
558 respective percentages of microbial reads from ITS or 16S amplicon sequencing.

559

560 **Microbial culture**

561 Microbes were cultured on MRS, YPD, PDA, or banana agar. MRS, YPD, and PDA were prepared
562 using MRS Broth (Merck Millipore), YPD medium (Clontech), and Potato Dextrose Broth
563 (Sigma-Aldrich), respectively, following the manufacturers' protocol. Banana agar was prepared
564 as previously described (Anagnostou et al., 2010), with the addition of autoclaving after making
565 the banana-agar mixture. 10% p-hydroxy-benzoic acid in 70% ethanol (prepared as described in
566 Kanaoka et al., 2023), propionic acid (Nacalai Tesque), cycloheximide (Wako), or ampicillin
567 (Nacalai Tesque) were added after autoclaving. Food-derived microbes were cultured at 25°C for
568 2 days, while *S. cerevisiae* was cultured at 30°C for 2 days before use, unless otherwise noted.

569 The *S. cerevisiae* BY4741 strain was obtained from NBRP-Yeast, Japan. To investigate
570 underlying mechanisms of differential growth-promoting ability between AAB and LAB, we
571 attempted to use *La. plantarum*^{WJL} and a genetically engineered BCAA-producing *Lacto*^{BCAA} strain
572 (B. Kim et al., 2021), both of which were kind gifts from W.-J. Lee. However, growth of *Lacto*^{BCAA}
573 strain on our banana agar was too slow, which made it impossible to obtain a sufficient quantity
574 of cells for the feeding experiments.

575

576 **Isolation and species identification of microbes**

577 Microbial strains were isolated on MRS, PDA, or banana-agar plates. The fermented foods were
578 spread on each of these plates. Single colonies were picked and re-streaked on a plate, and after

579 repeating the process once more, uniform colonies were collected, suspended in MRS liquid
580 medium containing 40% glycerol, and stored at -80°C.

581 To identify the species of each strain, PCR and sequencing were performed. Microbial
582 colonies were directly suspended in water in PCR tubes and heated (96°C for 5 min) before the
583 addition of other reagents. In the cases when DNA failed to amplify, DNA was extracted using
584 InstaGene Matrix (BIO-RAD) according to the manufacturer's protocol. NL1/NL4 primers were
585 used for fungi, while 27F/1492R primers were used for bacteria (Chandler et al., 2011, 2012). The
586 amplicon was purified prior to sequencing using a Wizard SV Gel and PCR Clean-Up System
587 (Promega).

588 Sequencing was performed using an Applied Biosystems 3130xl Genetic Analyzer, and
589 primers were NL1 for fungi and 518F (5'-CCAGCAGCCGCGGTAATACG-3') for bacteria
590 (https://www.macrogen-japan.co.jp/cap_seq_0104.php). See Table S3A for the sequencing results.

591 Species identification of isolated yeast strains was performed by NCBI BLAST searches
592 against the Nucleotide collection (nr/nt) database (Johnson et al., 2008). Sequences with Percent
593 Identity = 100%, E-value = 0 were considered as top hits, and the species name that appeared in
594 more than two top hits was used to refer to the strain. See also Table S3B for the number of the
595 top hits for each strain.

596 For bacteria, representative sequences of OTUs from the microbial composition analysis were
597 compared with the sequences of isolated strains, and the strain with the closest 16S rDNA sequence
598 was used as the strain corresponding to that OTU. See also Table S3C.

599

600 **Quantification of larval development**

601 The microbes were individually grown on banana agar twice before being suspended in PBS
602 (OD600 = 60). To mix multiple species, equal amounts of the suspensions prepared as described
603 were mixed together. 10 µL of each suspension was added to ~1.1 mL of autoclaved banana agar
604 in 1.5 mL tubes. Tubes were incubated at 25°C for 2 days before larvae were added. The following
605 procedure was performed as described in Watanabe et al., 2019, with a few modifications. Briefly,
606 20 germ-free larvae were added to each tube, and the tubes were kept in a moisturized incubator
607 (80-90% humidity) at 25°C. Pupariated individuals were removed from the tubes prior to eclosion,
608 and either discarded or transferred to vials for further incubation until eclosion occurred. The
609 number of pupae in each tube was counted until all larvae either pupariated or died. In experiments
610 that require daily addition of AAB, the bacterial cells (~3 mL by volume) were added daily except
611 for those days when the cells added the previous days were still visibly left.

612 The effect on larval development was quantified as the final percentage of the pupariated
613 individuals and timing of the pupariation. The developmental timing was quantified from the date
614 on which the percentage of pupariation exceeded 50% of the final percentage of pupariation. Molds
615 were occasionally seen on foods during incubation, in which case the tubes were removed from
616 the experiment. On a rare occasion when the number of samples for a single condition fell below
617 3, all the tubes for the condition were excluded from the results.

618

619 **Sequencing and annotation of yeast genomes**

620 To extract genomic DNA from yeast cells for genome sequencing, yeasts were cultured on MRS
621 plates. Collected cells were treated with Zymolyase-20T (Nacalai Tesque) to remove cell walls,
622 and DNA was extracted using QIAGEN Genomic-tip 20G kit (QIAGEN).

623 The genomic DNA prepared from six strains was sequenced by both Illumina and Oxford
624 Nanopore Technologies (ONT) technologies. For Illumina sequencing, libraries were prepared
625 with QIAseq FX DNA Library Kit (QIAGEN) and sequenced on the Illumina MiSeq platform
626 (Illumina, CA, USA) to generate 2 x 301 bp paired-end sequence reads. MiSeq reads were trimmed
627 using Platanus_trim (http://platanus.bio.titech.ac.jp/pltanus_trim). The thresholds for quality and
628 read length were set at 15 and 25, respectively. After trimming, a total of 1.863 - 2.396 Gb
629 sequence was obtained for each genome (average; 2.113 Gb). Sequence coverages estimated by
630 GenomeScope (Vurture et al., 2017) were over 100x for all genomes (103.42x - 210.48x). For
631 ONT sequencing, libraries were prepared with Rapid Barcoding Kit (ONT) and sequenced using
632 the R9.4.1 flow cell with the MinION platform, followed by base-calling using Albacore ver. 2.3.3.
633 (ONT). Adapter sequences of MinION reads were trimmed with NanoFilt (De Coster et al., 2018)
634 or Porechop (https://github.com/rrwick/Porechop), followed by filtering with a quality threshold
635 of 10 and a length threshold of 2000. After filtering, 84,598 - 197,215 reads (765 - 4,402 Mb in
636 total sequence length) were obtained for each genome (average; 121,913 reads and 1,035 Mb).
637 Estimated sequence coverages by MinION reads were 63.1x - 107.3x (average; 87.9x).

638 For RNA-seq analysis, equal amounts of yeast cells cultured under 6 conditions (2
639 temperatures: 25°C and 30°C, and 3 culture plates: MRS, YPD, or banana-agar plates) were mixed
640 and used for RNA extraction. RNA was extracted as previously described (Iida & Kobayashi,
641 2019) and purified using the RNeasy mini kit (QIAGEN). Libraries for RNA-seq were prepared
642 with NEBNext Ultra II Directional RNA Library Prep Kit for Illumina (NEB) and sequenced on
643 the NextSeq 500 platform (Illumina) to generate 300-base paired end sequences which were used
644 for annotation described below. A total of 23.48-26.75M reads were obtained for each yeast
645 (average; 25.63M reads).

646 Genome assembly was performed by MaSuRCA v3.2.6 (Zimin et al., 2013) using MiSeq and
647 MinION reads. In the heterozygosity rate estimation by GenomeScope based on MiSeq reads, the
648 *Kazachstania humilis* and *Pichia kluyveri* genomes showed higher heterozygosity rates (*K.*
649 *humilis* ; 2.98% , *Pi. kluyveri*; 2.08%) while those of other genomes were 0.02% - 1,00%. In the
650 assessment of autoannotated genome assemblies using BUSCO (Simão et al., 2015), completeness
651 was over 86% in the four genomes other than the *H. uvarum* (64.58%) and *St. bacillaris* (75.21%)
652 genomes. However, among the four genomes, those of *Pi. kluyveri* and *K. humilis* showed a high
653 proportion of "Duplicated complete" genes (*K. humilis*; 27.74%, *Pi. kluyveri*; 5.17%, respectively),
654 which was apparently due to the high heterozygosity rate of these genomes. Therefore, these two
655 genomes were assembled using Platanus-allee v2.2.2 (Kajitani et al., 2019), and by comparing it
656 with the MaSuRCA assemblies using GenomeMatcher (Ohtsubo et al., 2008), redundant
657 sequences in the MaSuRCA assemblies were identified and removed from the assemblies. As the
658 proportions of "Duplicated complete" genes estimated by BUSCO were 5.51% for the *K. humilis*
659 genome and 0.74% for the *Pi. kluyveri* genome after removing redundant sequences, these
660 redundant sequence-removed genome assemblies were used as the final genome assemblies of *Pi.*
661 *kluyveri* and *K. humilis*.

662 Genome annotation was performed using FunGAP (Min et al., 2017) with the above-mentioned
663 RNA-seq data obtained from each yeast. Over 91% of RNA-seq reads obtained was mapped to the
664 final assemblies of each genome using Hisat2 (D. Kim et al., 2015). In the assessment of annotated
665 genomes using BUSCO, completeness was >86% for the four genomes other than those of *H.*
666 *uvarum* (65.95%) and *St. bacillaris* (76.92%). It appears thtat he low completeness of these
667 genomes are attributable to genome reduction. The final statuses of genome assembly and
668 annotation of each genome are summarized in Supplementary Table S7.

669 Mitochondrial sequences in each genome assembly were identified by tblastx homology search
670 with fungal mitochondrial sequences obtained from the RefSeq database (O'Leary et al., 2016).
671 When multimerized mitochondrial sequences were generated in genome assemblies, they were
672 trimmed to the smallest unit.

673 To determine gene orthology between *S. cerevisiae* and each of the isolated strains, blastp was
674 performed. *S. cerevisiae* protein sequence data (GCF_000146045.2_R64_protein.faa) was
675 downloaded from NCBI genome database (https://www.ncbi.nlm.nih.gov/genome). Reciprocal
676 best hits with an e-value < 10^{-10} were defined as orthologs.

677

678 **Quantification of AAB**

679 Microbes were inoculated onto 200 mL of banana agar in a tube included in a Biomasher II
680 homogenizer kit (Funakoshi). After adding 5 germ-free larvae, the tubes were incubated at 25°C
681 for 4 days. 150 µL of PBS was added to the tube, and food was crushed along with the larvae in it.
682 More PBS was subsequently added to bring the total volume of the suspension to 700 µL. 1/5
683 serial dilutions were made, 50 µL of which were spread onto MRS plates supplemented with
684 antibiotics (10 µg/mL cycloheximide and 10 µg/mL ampicillin to inhibit the growth of yeasts and
685 LAB, respectively). The plates were incubated at 25°C, and 2 days later, colonies were counted to
686 calculate CFU.

687

688 **RNA sequencing for gene expression analyses**

689 For larval RNA-seq analysis, microbes were inoculated on banana agar as previously described
690 and freshly hatched germ-free larvae were added. After 15 h feeding, 20 larvae were collected and
691 snap-frozen. RNA extraction, sequencing, and data analysis were performed as previously
692 described (Kanaoka et al., 2023).

693 Yeast RNA was extracted as described above, and sequenced as previously described in Kanaoka
694 et al., 2023. Data obtained from the FunGAP analysis were used for mapping of reads obtained for
695 the isolated strains, and the *S. cerevisiae* S288C genome R64-1-1, retrieved from Illumina
696 iGenomes (https://jp.support.illumina.com/sequencing/sequencing_software/igenome.html) for *S.*
697 *cerevisiae* BY4741.

698 For the heatmaps in Figures 3A and 4C, heatmap.2 in the gplots (Warnes et al., 2022) package
699 of R (R Core Team, 2020) was used. Database for annotation, visualization and integrated
700 discovery (DAVID) Functional Annotation Chart (Huang et al., 2009; Sherman et al., 2022) was
701 used to find significantly enriched GO terms or KEGG Pathways in each analysis. For comparisons
702 with the microarray analysis result of Zinke et al., 2002, their gene expression data of the

703 individuals at 12 h after feeding or starvation was used. Genes that were represented by more than
704 one probes were omitted. The FlyBase IDs in the data of Zinke et al., 2002 were converted to
705 current IDs using FlyBase ID Validator (https://flybase.org/convert/id). Only the genes that had
706 one-to-one correspondence with current FlyBase IDs were included in the heat maps.

707

708 **Preparing samples for LC-MS analysis**

709 The yeasts were individually grown on banana agar three times. 100 mg of cells were scraped from
710 the surface of the plates and snap-frozen. To prepare yeast-conditioned plates, yeasts were grown
711 as described and thoroughly removed by scraping; in addition, 22 mm^2 chunks of agar from the
712 plates (~100-160 mg) were collected and snap-frozen. 15 g/L agar plates or sterile banana-agar
713 plates were prepared as controls and collected using the same procedure. To prepare cell
714 suspension supernatants, ~250 mg of yeast cells were collected as described, and sterile PBS was
715 added at a ratio of 5 µL PBS per 1 mg of yeast cells. After suspending the cells, the suspensions
716 were centrifuged at 5,000 rpm for 5 min. The supernatants were further filtered using a 0.45 µm
717 Millex-HA filter (Merck) to completely remove any remaining yeast cells. 700 µL of each
718 supernatant was collected and snap-frozen.

719 Each sample was suspended or diluted to 500 µL of methanol containing internal standard;
720 100 mM MES and 100 mM L-Met. After mixing with 250 µL of water and 400 µL of chloroform,
721 the samples were centrifuged and the upper layer was collected and filtered using an UltrafreeMC-
722 PLHCC for Metabolome Analysis column (Human Metabolome Technologies, #UFC3LCCNB-
723 HMT). The samples were dried completely using nitrogen gas and resuspended in water before
724 injection into the LC-MS system.

725

726 **LC-MS/MS measurement**

727 Cationic metabolites including amino acids and nucleosides are quantified using a triple-
728 quadrupole mass spectrometer equipped with an electrospray ionization (ESI) ion source (LCMS-
729 8060, Shimadzu Corporation) in the positive and negative-ESI and multiple reaction monitoring
730 (MRM) modes. The samples were resolved on the Discovery HS F5-3 column (2.1 mm ID × 150
731 mm, 3-µm particle, Sigma-Aldrich), using a step gradient with mobile phase A (0.1% formate /
732 water) and mobile phase B (0.1% formate /acetonitrile) at ratios of 100:0 (0–5 min), 75:25 (5–11
733 min), 65:35 (11–15 min), 5:95 (15–20 min) and 100:0 (20–25 min), at a flow rate of 0.25 ml min
734 −1 and a column temperature of 40°C.

735 Data are presented as peak area values for each metabolite normalized by the internal standard.
736 Those for the yeast-conditioned plates or cells were further normalized with sample wet weight.
737 Heat maps were generated by MetaboAnalystR 3.3.0. (Pang et al., 2020), using data for all of the
738 detected metabolites or a subset of metabolites that is included in the holidic medium of
739 *Drosophila melanogaster* (Piper et al., 2014).

740

741 **Developmental progression with BCAA supplementation**

742 Yeasts were cultured as described on autoclaved banana agar supplemented with 2.03 g/L of
743 leucine (Nacalai Tesque) and 1.12 g/L of isoleucine (Peptide Institute), both at the concentrations
744 included in the holidic medium with exome-matched FLYAA (Piper et al., 2017). 20 larvae were
745 added to each tube, and after 11 days of feeding, live or dead individuals in each developmental
746 stage were counted. Larval developmental stages were determined based on tracheal morphology,
747 as previously described (Niwa et al., 2010). The percentage of the larvae that could not be found
748 are indicated as "Not found."

749

750 **Imaging of dead yeast cells**

751 Microbes were collected from banana-agar plates, suspended in PBS at a concentration of ~1x 10^8
752 cells/mL, and incubated in 5 µg/mL Phloxine B (Wako) for 10 min at room temperature. The cells
753 were subsequently washed twice with PBS and observed using a Nikon C1 laser scanning confocal
754 microscope coupled to a Nikon Eclipse E-800 microscope. Note that the brightness of the images
755 was adjusted with a gradation to achieve mostly uniform brightness, because the bottom side of
756 the original images was darker due to microscope malfunction.

757

758 **Statistical analysis**

759 R (R Core Team, 2020) was used for all statistical analyses. P-values less than 0.05 were
760 considered statistically significant. For statistical analyses of RNA-seq data, see Tables S4, S5,
761 and S8. See Table S9, Materials and Methods, and figure legends for analysis of other experiments.

762

763 **Data availability**

764 All sequence data obtained in this study have been deposited in the DDBJ Sequence Read Archive.
765 The accession numbers for the data are DRR212820-DRR212838 (BioProject accession number:
766 PRJDB9099) and DRR471830-DRR471964 (BioProject accession number: PRJDB15711).
767

ACKNOWLEDGMENTS

We thank T. Kondo and Y. Sando for performing RNA sequencing; M. Umeda and T. Suito for technical advice on microbial isolation and identification; K. Furuya for technical advice on yeast genomic DNA extraction and Phloxine B staining; T. Iida and T. Kobayashi for technical advice on yeast RNA extraction; J. Hejna for polishing the manuscript; H. Imai, K. Oki, and M. Futamata for technical and secretarial assistance; T. Kuraishi, A. Hori, Y. Degawa, Y. Yoshihashi, R. Niwa, T. Ito for technical advice and discussion; W.-J. Lee for providing bacterial strains; and members of the Uemura laboratory for technical advice, discussion, and kind cooperation in obtaining fermented food samples. This work was supported by the Japan Society for the Promotion of Science (JSPS; 21K06186, 17K15039 and 16H06279 [PAGS] to Y.H., 17KT0018 to T.U., and 20J23332 to A.M.); AMED-CREST (JP18gm1110001 to T.U.); and JST FOREST Program (JPMJFR2051 to Y.H.).

COMPETING INTERESTS

The authors declare no competing interests.

REFERENCES

Anagnostou, C., Dorsch, M., & Rohlfs, M. (2010). Influence of dietary yeasts on Drosophila melanogaster life-history traits. Entomologia Experimentalis et Applicata, 136(1), 1–11. https://doi.org/10.1111/j.1570-7458.2010.00997.x

Asha, H., Nagy, I., Kovacs, G., Stetson, D., Ando, I., & Dearolf, C. R. (2003). Analysis of Ras-induced overproliferation in Drosophila hemocytes. Genetics, 163(1), 203–215.

Baumberger, J. P. (1917). The Food of Drosophila Melanogaster Meigen. Proceedings of the National Academy of Sciences of the United States of America, 3(2), 122–126. https://doi.org/10.1073/pnas.3.2.122

Broderick, N. A., & Lemaitre, B. (2012). Gut-associated microbes of Drosophila melanogaster. Gut Microbes, 3(4), 307–321. https://doi.org/10.4161/gmic.19896

Caporaso, J. G., Kuczynski, J., Stombaugh, J., Bittinger, K., Bushman, F. D., Costello, E. K., Fierer, N., Peña, A. G., Goodrich, J. K., Gordon, J. I., Huttley, G. A., Kelley, S. T., Knights, D., Koenig, J. E., Ley, R. E., Lozupone, C. A., McDonald, D., Muegge, B. D., Pirrung, M., … Knight, R. (2010). QIIME allows analysis of high-throughput community sequencing data. Nature Methods, 7(5), 335–336. https://doi.org/10.1038/nmeth.f.303

Chandler, J. A., Eisen, J. A., & Kopp, A. (2012). Yeast communities of diverse Drosophila species: Comparison of two symbiont groups in the same hosts. Applied and Environmental Microbiology, 78(20), 7327–7336. https://doi.org/10.1128/AEM.01741-12

Chandler, J. A., Lang, J., Bhatnagar, S., Eisen, J. A., & Kopp, A. (2011). Bacterial communities of diverse Drosophila species: Ecological context of a host-microbe model system. PLoS Genetics, 7(9), e1002272. https://doi.org/10.1371/journal.pgen.1002272

Cole, J. R., Wang, Q., Fish, J. A., Chai, B., McGarrell, D. M., Sun, Y., Brown, C. T., Porras-Alfaro, A., Kuske, C. R., & Tiedje, J. M. (2014). Ribosomal Database Project: Data and tools for high throughput rRNA analysis. Nucleic Acids Research, 42(Database issue), D633–D642. https://doi.org/10.1093/nar/gkt1244

Coluccio, A. E., Rodriguez, R. K., Kernan, M. J., & Neiman, A. M. (2008). The Yeast Spore Wall Enables Spores to Survive Passage through the Digestive Tract of Drosophila. PLoS ONE, 3(8), e2873. https://doi.org/10.1371/journal.pone.0002873

Consuegra, J., Grenier, T., Akherraz, H., Rahioui, I., Gervais, H., da Silva, P., & Leulier, F. (2020). Metabolic Cooperation among Commensal Bacteria Supports Drosophila Juvenile Growth under Nutritional Stress. IScience, 23(6), 101232. https://doi.org/10.1016/j.isci.2020.101232

Consuegra, J., Grenier, T., Baa-Puyoulet, P., Rahioui, I., Akherraz, H., Gervais, H., Parisot, N., da Silva, P., Charles, H., Calevro, F., & Leulier, F. (2020). Drosophila-associated bacteria differentially shape the nutritional requirements of their host during juvenile growth. PLOS Biology, 18(3), e3000681. https://doi.org/10.1371/journal.pbio.3000681

Corby-Harris, V., Pontaroli, A. C., Shimkets, L. J., Bennetzen, J. L., Habel, K. E., & Promislow, D. E. L. (2007). Geographical Distribution and Diversity of Bacteria Associated with Natural Populations of Drosophila melanogaster. Applied and Environmental Microbiology, 73(11), 3470–3479. https://doi.org/10.1128/AEM.02120-06

825 Cox, C. R., & Gilmore, M. S. (2007). Native Microbial Colonization of Drosophila melanogaster
826 and Its Use as a Model of Enterococcus faecalis Pathogenesis. Infection and Immunity, 75(4),
827 1565–1576. https://doi.org/10.1128/IAI.01496-06

828 De Coster, W., D'Hert, S., Schultz, D. T., Cruts, M., & Van Broeckhoven, C. (2018). NanoPack:
829 Visualizing and processing long-read sequencing data. Bioinformatics, 34(15), 2666–2669.
830 https://doi.org/10.1093/bioinformatics/bty149

831 Fox, H. L., Pham, P. T., Kimball, S. R., Jefferson, L. S., & Lynch, C. J. (1998). Amino acid
832 effects on translational repressor 4E-BP1 are mediated primarily by l-leucine in isolated
833 adipocytes. American Journal of Physiology, 275(5), C1232–C1238.
834 https://doi.org/10.1152/ajpcell.1998.275.5.C1232

835 Gallo, M., Vento, J. M., Joncour, P., Quagliariello, A., Maritan, E., Silva-Soares, N. F.,
836 Battistolli, M., Beisel, C. L., & Martino, M. E. (2022). Beneficial commensal bacteria promote
837 Drosophila growth by downregulating the expression of peptidoglycan recognition proteins.
838 IScience, 25(6), 104357. https://doi.org/10.1016/j.isci.2022.104357

839 Grenier, T., & Leulier, F. (2020). How commensal microbes shape the physiology of Drosophila
840 melanogaster. Current Opinion in Insect Science, 41, 92–99.
841 https://doi.org/10.1016/j.cois.2020.08.002

842 Gu, X., Jouandin, P., Lalgudi, P. V., Binari, R., Valenstein, M. L., Reid, M. A., Allen, A. E.,
843 Kamitaki, N., Locasale, J. W., Perrimon, N., & Sabatini, D. M. (2022). Sestrin mediates
844 detection of and adaptation to low-leucine diets in Drosophila. Nature, 608(7921), Article 7921.
845 https://doi.org/10.1038/s41586-022-04960-2

846 Hallen-Adams, H. E., & Suhr, M. J. (2017). Fungi in the healthy human gastrointestinal tract.
847 Virulence, 8(3), 352–358. https://doi.org/10.1080/21505594.2016.1247140

848 Henriques, S. F., Dhakan, D. B., Serra, L., Francisco, A. P., Carvalho-Santos, Z., Baltazar, C.,
849 Elias, A. P., Anjos, M., Zhang, T., Maddocks, O. D. K., & Ribeiro, C. (2020). Metabolic cross-
850 feeding in imbalanced diets allows gut microbes to improve reproduction and alter host
851 behaviour. Nature Communications, 11(1), 4236. https://doi.org/10.1038/s41467-020-18049-9

852 Hoang, D., Kopp, A., & Chandler, J. A. (2015). Interactions between Drosophila and its natural
853 yeast symbionts-Is Saccharomyces cerevisiae a good model for studying the fly-yeast
854 relationship? PeerJ, 3, e1116. https://doi.org/10.7717/peerj.1116

855 Hoshino, Y., & Gaucher, E. A. (2021). Evolution of bacterial steroid biosynthesis and its impact
856 on eukaryogenesis. Proceedings of the National Academy of Sciences, 118(25), e2101276118.
857 https://doi.org/10.1073/pnas.2101276118

858 Huang, D. W., Sherman, B. T., & Lempicki, R. A. (2009). Systematic and integrative analysis of
859 large gene lists using DAVID bioinformatics resources. Nature Protocols, 4(1), Article 1.
860 https://doi.org/10.1038/nprot.2008.211

861 Hugerth, L. W., Wefer, H. A., Lundin, S., Jakobsson, H. E., Lindberg, M., Rodin, S., Engstrand,
862 L., & Andersson, A. F. (2014). DegePrime, a program for degenerate primer design for broad-
863 taxonomic-range PCR in microbial ecology studies. Applied and Environmental Microbiology,
864 80(16), 5116–5123. https://doi.org/10.1128/AEM.01403-14

Iida, T., & Kobayashi, T. (2019). RNA Polymerase I Activators Count and Adjust Ribosomal RNA Gene Copy Number. Molecular Cell, 73(4), 645–654. https://doi.org/10.1016/j.molcel.2018.11.029

Ikeda-Ohtsubo, W., Brugman, S., Warden, C. H., Rebel, J. M. J., Folkerts, G., & Pieterse, C. M. J. (2018). How Can We Define "Optimal Microbiota?": A Comparative Review of Structure and Functions of Microbiota of Animals, Fish, and Plants in Agriculture. Frontiers in Nutrition, 5, 90.

Johnson, M., Zaretskaya, I., Raytselis, Y., Merezhuk, Y., McGinnis, S., & Madden, T. L. (2008). NCBI BLAST: A better web interface. Nucleic Acids Research, 36(Web Server issue), W5-9. https://doi.org/10.1093/nar/gkn201

Kajitani, R., Yoshimura, D., Okuno, M., Minakuchi, Y., Kagoshima, H., Fujiyama, A., Kubokawa, K., Kohara, Y., Toyoda, A., & Itoh, T. (2019). Platanus-allee is a de novo haplotype assembler enabling a comprehensive access to divergent heterozygous regions. Nature Communications, 10(1), 1702. https://doi.org/10.1038/s41467-019-09575-2

Kanaoka, Y., Onodera, K., Watanabe, K., Hayashi, Y., Usui, T., Uemura, T., & Hattori, Y. (2023). Inter-organ Wingless/Ror/Akt signaling regulates nutrient-dependent hyperarborization of somatosensory neurons. ELife, 12, e79461. https://doi.org/10.7554/eLife.79461

Kim, B., Kanai, M. I., Oh, Y., Kyung, M., Kim, E.-K., Jang, I.-H., Lee, J.-H., Kim, S.-G., Suh, G. S. B., & Lee, W.-J. (2021). Response of the microbiome–gut–brain axis in Drosophila to amino acid deficit. Nature, 593(7860), Article 7860. https://doi.org/10.1038/s41586-021-03522-2

Kim, D., Langmead, B., & Salzberg, S. L. (2015). HISAT: A fast spliced aligner with low memory requirements. Nature Methods, 12(4), 357–360. https://doi.org/10.1038/nmeth.3317

Kim, J., & Guan, K.-L. (2019). MTOR as a central hub of nutrient signalling and cell growth. Nature Cell Biology, 21(1), Article 1. https://doi.org/10.1038/s41556-018-0205-1

Kwong, W. K., & Moran, N. A. (2013). Cultivation and characterization of the gut symbionts of honey bees and bumble bees: Description of Snodgrassella alvi gen. nov., sp. nov., a member of the family Neisseriaceae of the Betaproteobacteria, and Gilliamella apicola gen. nov., sp. nov., a member of Orbaceae fam. nov., Orbales ord. nov., a sister taxon to the order 'Enterobacteriales' of the Gammaproteobacteria. International Journal of Systematic and Evolutionary Microbiology, 63(Pt_6), 2008–2018. https://doi.org/10.1099/ijs.0.044875-0

Lee, W.-J., & Brey, P. T. (2013). How microbiomes influence metazoan development: Insights from history and Drosophila modeling of gut-microbe interactions. Annual Review of Cell and Developmental Biology, 29(1), 571–592. https://doi.org/10.1146/annurev-cellbio-101512-122333

Lofgren, L. A., Uehling, J. K., Branco, S., Bruns, T. D., Martin, F., & Kennedy, P. G. (2019). Genome-based estimates of fungal rDNA copy number variation across phylogenetic scales and ecological lifestyles. Molecular Ecology, 28(4), 721–730. https://doi.org/10.1111/mec.14995

Ludington, W. B., & Ja, W. W. (2020). Drosophila as a model for the gut microbiome. PLOS Pathogens, 16(4), e1008398. https://doi.org/10.1371/journal.ppat.1008398

Magoč, T., & Salzberg, S. L. (2011). FLASH: Fast length adjustment of short reads to improve genome assemblies. Bioinformatics, 27(21), 2957–2963. https://doi.org/10.1093/bioinformatics/btr507

Martino, M. E., Joncour, P., Leenay, R., Gervais, H., Shah, M., Hughes, S., Gillet, B., Beisel, C., & Leulier, F. (2018). Bacterial Adaptation to the Host's Diet Is a Key Evolutionary Force Shaping Drosophila-Lactobacillus Symbiosis. Cell Host & Microbe, 24(1), 109–119. https://doi.org/10.1016/j.chom.2018.06.001

Min, B., Grigoriev, I. V., & Choi, I.-G. (2017). FunGAP: Fungal Genome Annotation Pipeline using evidence-based gene model evaluation. Bioinformatics, 33(18), 2936–2937. https://doi.org/10.1093/bioinformatics/btx353

Moya, A., & Ferrer, M. (2016). Functional Redundancy-Induced Stability of Gut Microbiota Subjected to Disturbance. Trends in Microbiology, 24(5), 402–413. https://doi.org/10.1016/j.tim.2016.02.002

Nilsson, R. H., Larsson, K.-H., Taylor, A. F. S., Bengtsson-Palme, J., Jeppesen, T. S., Schigel, D., Kennedy, P., Picard, K., Glöckner, F. O., Tedersoo, L., Saar, I., Kõljalg, U., & Abarenkov, K. (2019). The UNITE database for molecular identification of fungi: Handling dark taxa and parallel taxonomic classifications. Nucleic Acids Research, 47(D1), D259–D264. https://doi.org/10.1093/nar/gky1022

Niwa, R., Namiki, T., Ito, K., Shimada-Niwa, Y., Kiuchi, M., Kawaoka, S., Kayukawa, T., Banno, Y., Fujimoto, Y., Shigenobu, S., Kobayashi, S., Shimada, T., Katsuma, S., & Shinoda, T. (2010). Non-molting glossy / shroud encodes a short-chain dehydrogenase/reductase that functions in the 'Black Box' of the ecdysteroid biosynthesis pathway. Development, 137(12), 1991–1999. https://doi.org/10.1242/dev.045641

Ohtsubo, Y., Ikeda-Ohtsubo, W., Nagata, Y., & Tsuda, M. (2008). GenomeMatcher: A graphical user interface for DNA sequence comparison. BMC Bioinformatics, 9(376). https://doi.org/10.1186/1471-2105-9-376

O'Leary, N. A., Wright, M. W., Brister, J. R., Ciufo, S., Haddad, D., McVeigh, R., Rajput, B., Robbertse, B., Smith-White, B., Ako-Adjei, D., Astashyn, A., Badretdin, A., Bao, Y., Blinkova, O., Brover, V., Chetvernin, V., Choi, J., Cox, E., Ermolaeva, O., … Pruitt, K. D. (2016). Reference sequence (RefSeq) database at NCBI: Current status, taxonomic expansion, and functional annotation. Nucleic Acids Research, 44(D1), D733–D745. https://doi.org/10.1093/nar/gkv1189

Oyewole, O. A. (2012). Microorganisms associated with deterioration of stored banana fruits. Frontiers in Science, 2(5), 86–91. https://doi.org/10.5923/j.fs.20120205.01

Pais, I. S., Valente, R. S., Sporniak, M., & Teixeira, L. (2018). Drosophila melanogaster establishes a species-specific mutualistic interaction with stable gut-colonizing bacteria. PLOS Biology, 16(7), e2005710. https://doi.org/10.1371/journal.pbio.2005710

Pang, Z., Chong, J., Li, S., & Xia, J. (2020). MetaboAnalystR 3.0: Toward an Optimized Workflow for Global Metabolomics. Metabolites, 10(5), Article 5. https://doi.org/10.3390/metabo10050186

Pérez, J. C. (2021). Fungi of the human gut microbiota: Roles and significance. International Journal of Medical Microbiology, 311(3), 151490. https://doi.org/10.1016/j.ijmm.2021.151490

Piper, M. D. W., Blanc, E., Leitão-Gonçalves, R., Yang, M., He, X., Linford, N. J., Hoddinott, M. P., Hopfen, C., Soultoukis, G. A., Niemeyer, C., Kerr, F., Pletcher, S. D., Ribeiro, C., &

Partridge, L. (2014). A holidic medium for Drosophila melanogaster. Nature Methods, 11(1), 100–105. https://doi.org/10.1038/nmeth.2731

Piper, M. D. W., Soultoukis, G. A., Blanc, E., Mesaros, A., Herbert, S. L., Juricic, P., He, X., Atanassov, I., Salmonowicz, H., Yang, M., Simpson, S. J., Ribeiro, C., & Partridge, L. (2017). Matching Dietary Amino Acid Balance to the In Silico-Translated Exome Optimizes Growth and Reproduction without Cost to Lifespan. Cell Metabolism, 25(3), 610–621. https://doi.org/10.1016/j.cmet.2017.02.005

Qiu, X., Yu, L., Wang, W., Yan, R., Zhang, Z., Yang, H., Zhu, D., & Zhu, B. (2021). Comparative Evaluation of Microbiota Dynamics and Metabolites Correlation Between Spontaneous and Inoculated Fermentations of Nanfeng Tangerine Wine. Frontiers in Microbiology, 12, 649978.

Quan, A. S., & Eisen, M. B. (2018). The ecology of the drosophila-yeast mutualism in wineries. PLOS ONE, 13(5), e0196440. https://doi.org/10.1371/journal.pone.0196440

R Core Team. (2020). R: A Language and Environment for Statistical Computing. R Foundation for Statistical Computing. https://www.R-project.org/

Sherman, B. T., Hao, M., Qiu, J., Jiao, X., Baseler, M. W., Lane, H. C., Imamichi, T., & Chang, W. (2022). DAVID: A web server for functional enrichment analysis and functional annotation of gene lists (2021 update). Nucleic Acids Research, 50(W1), W216–W221. https://doi.org/10.1093/nar/gkac194

Shigenobu, S., & Wilson, A. C. C. (2011). Genomic revelations of a mutualism: The pea aphid and its obligate bacterial symbiont. Cellular and Molecular Life Sciences, 68(8), 1297–1309. https://doi.org/10.1007/s00018-011-0645-2

Shihata, A. M. E.-T. A., & Mrak, E. M. (1952). Intestinal Yeast Floras of Successive Populations of Drosophila. Evolution, 6, 325–332. https://doi.org/10.1111/j.1558-5646.1952.tb01428.x

Shin, S. C., Kim, S. H., You, H., Kim, B., Kim, A. C., Lee, K. A., Yoon, J. H., Ryu, J. H., & Lee, W. J. (2011). Drosophila microbiome modulates host developmental and metabolic homeostasis via insulin signaling. Science, 334(6056), 670–674. https://doi.org/10.1126/science.1212782

Simão, F. A., Waterhouse, R. M., Ioannidis, P., Kriventseva, E. V., & Zdobnov, E. M. (2015). BUSCO: Assessing genome assembly and annotation completeness with single-copy orthologs. Bioinformatics, 31(19), 3210–3212. https://doi.org/10.1093/bioinformatics/btv351

Solomon, G. M., Dodangoda, H., McCarthy-Walker, T. T., Ntim-Gyakari, R. R., & Newell, P. D. (2019). The microbiota of Drosophila suzukii influences the larval development of Drosophila melanogaster. PeerJ, 7, e8097. https://doi.org/10.7717/peerj.8097

Stamps, J. A., Yang, L. H., Morales, V. M., & Boundy-Mills, K. L. (2012). Drosophila regulate yeast density and increase yeast community similarity in a natural substrate. PLoS ONE, 7(7), e42238. https://doi.org/10.1371/journal.pone.0042238

Stoddard, S. F., Smith, B. J., Hein, R., Roller, B. R. K., & Schmidt, T. M. (2015). rrnDB: Improved tools for interpreting rRNA gene abundance in bacteria and archaea and a new foundation for future development. Nucleic Acids Research, 43(D1), D593–D598. https://doi.org/10.1093/nar/gku1201

988 Storelli, G., Defaye, A., Erkosar, B., Hols, P., Royet, J., & Leulier, F. (2011). Lactobacillus
989 plantarum Promotes Drosophila Systemic Growth by Modulating Hormonal Signals through
990 TOR-Dependent Nutrient Sensing. Cell Metabolism, 14(3), 403–414.
991 https://doi.org/10.1016/j.cmet.2011.07.012

992 Su, Y., Lin, H.-C., Teh, L. S., Chevance, F., James, I., Mayfield, C., Golic, K. G., Gagnon, J. A.,
993 Rog, O., & Dale, C. (2022). Rational engineering of a synthetic insect-bacterial mutualism.
994 Current Biology, 32(18), 3925–3938. https://doi.org/10.1016/j.cub.2022.07.036

995 Vurture, G. W., Sedlazeck, F. J., Nattestad, M., Underwood, C. J., Fang, H., Gurtowski, J., &
996 Schatz, M. C. (2017). GenomeScope: Fast reference-free genome profiling from short reads.
997 Bioinformatics, 33(14), 2202–2204. https://doi.org/10.1093/bioinformatics/btx153

998 Warnes, G. R., Bolker, B., Bonebakker, L., Gentleman, R., Huber, W., Liaw, A., Lumley, T.,
999 Maechler, M., Magnusson, A., Moeller, S., Schwartz, M., & Venables, B. (2022). gplots:
1000 Various R Programming Tools for Plotting Data. https://CRAN.R-project.org/package=gplots

1001 Watanabe, K., Furumizo, Y., Usui, T., Hattori, Y., & Uemura, T. (2017). Nutrient-dependent
1002 increased dendritic arborization of somatosensory neurons. Genes to Cells, 22(1), 105–114.
1003 https://doi.org/10.1111/gtc.12451

1004 Watanabe, K., Kanaoka, Y., Mizutani, S., Uchiyama, H., Yajima, S., Watada, M., Uemura, T., &
1005 Hattori, Y. (2019). Interspecies comparative analyses reveal distinct carbohydrate-responsive
1006 systems among Drosophila species. Cell Reports, 28(10), 2594–2607.
1007 https://doi.org/10.1016/j.celrep.2019.08.030

1008 Werren, J. H., Windsor, D., & Guo, L. (1995). Distribution of Wolbachia among Neotropical
1009 Arthropods. Proceedings: Biological Sciences, 262(1364), 197–204.

1010 White, T. J., Bruns, T., Lee, S., & Taylor, J. (1990). Amplification and direct sequencing of
1011 fungal ribosomal RNA genes for phylogenetics. In PCR protocols: A guide to methods and
1012 applications (Vol. 18, pp. 315–322). Academic Press.

1013 Zhang, S., Lin, X., Hou, Q., Hu, Z., Wang, Y., & Wang, Z. (2021). Regulation of mTORC1 by
1014 amino acids in mammalian cells: A general picture of recent advances. Animal Nutrition, 7(4),
1015 1009–1023. https://doi.org/10.1016/j.aninu.2021.05.003

1016 Zheng, D., Liwinski, T., & Elinav, E. (2020). Interaction between microbiota and immunity in
1017 health and disease. Cell Research, 30(6), Article 6. https://doi.org/10.1038/s41422-020-0332-7

1018 Zimin, A. V., Marçais, G., Puiu, D., Roberts, M., Salzberg, S. L., & Yorke, J. A. (2013). The
1019 MaSuRCA genome assembler. Bioinformatics, 29(21), 2669–2677.
1020 https://doi.org/10.1093/bioinformatics/btt476

1021 Zinke, I., Schütz, C. S., Katzenberger, J. D., Bauer, M., & Pankratz, M. J. (2002). Nutrient
1022 control of gene expression in Drosophila: Microarray analysis of starvation and sugar-dependent
1023 response. The EMBO Journal, 21(22), 6162–6173. https://doi.org/10.1093/emboj/cdf600

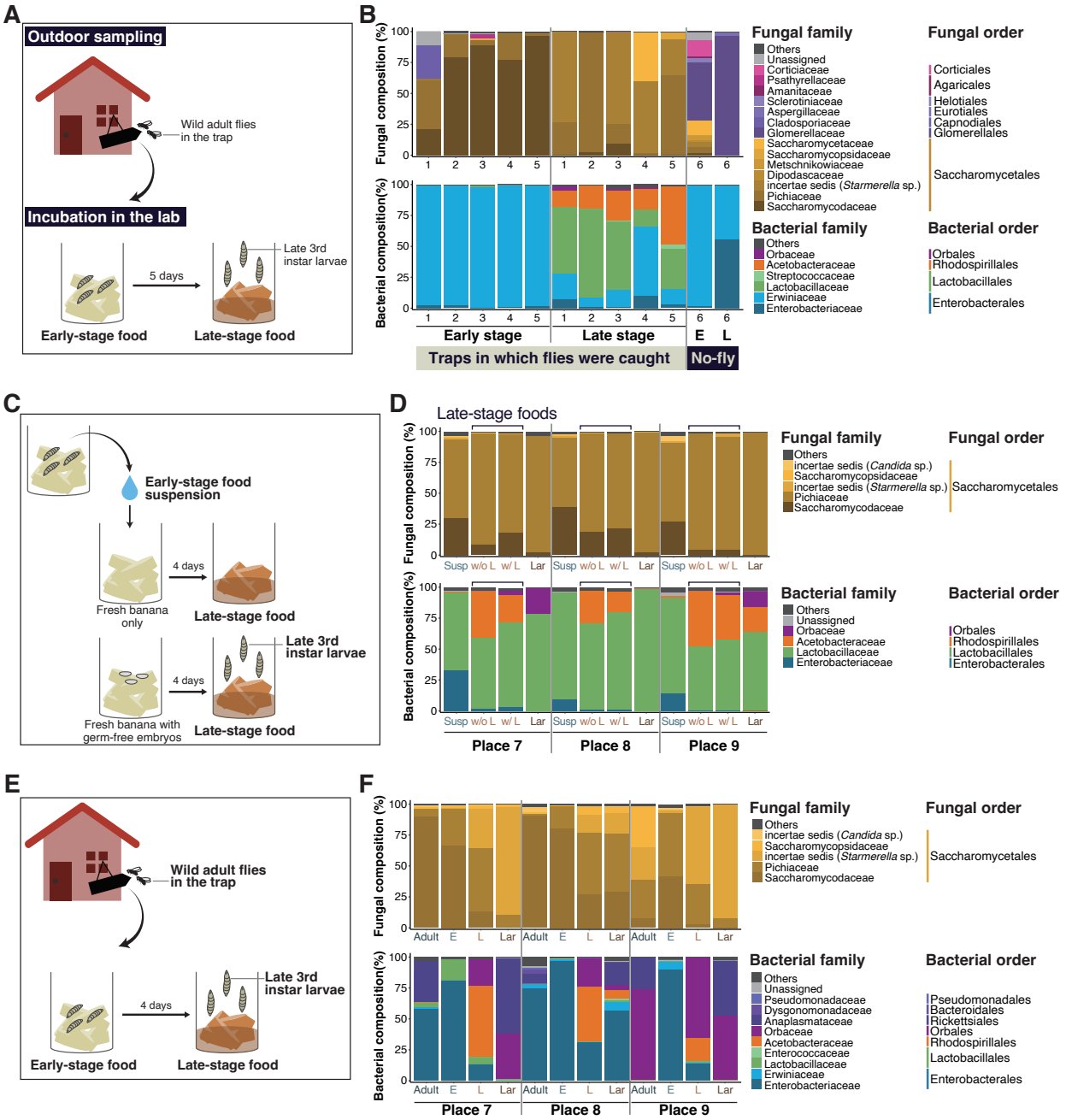

1024 Figure 1. Mure et al.

1025 **Figure 1. The composition of both yeast and bacteria in the food microbiota shifts as**
1026 **fermentation progresses, independently of the presence of larvae**

1027 (A-F) Sampling designs and results for the analyses of microbial compositions in natural food
1028 sources of *Drosophila* (A and B), effects of larval presence on the microbial composition shift (C
1029 and D), or microbial compositions in adult flies, larvae, and their foods (E and F). (A, C, and E)
1030 Designs of the samplings for microbial analyses. Traps with bananas were set up outdoors near
1031 human habitations in order to collect samples on which wild *Drosophila* spp. lay eggs. Fermented
1032 food samples were collected from the traps at two time points: the early stage (just after trap
1033 collection), and the late stage (when larvae in the foods developed into late 3rd instars). Collected
1034 samples are indicated in bold letters. (C) In this sampling, the collected early-stage food was
1035 crushed in PBS, and the liquid portion (microbial suspension) was added to fresh bananas with or
1036 without germ-free embryos (*Cg-Gal4, UAS-mCD8:GFP*). After incubation, late-stage food and
1037 surface-sterilized larvae were collected. (E) In addition to the food samples, adult flies in the traps
1038 and larvae from the late-stage foods were collected. This sampling was conducted independently
1039 from that shown in (C) and (D), although the sampling places were in common. Both adults and
1040 larvae were surface-sterilized. Note that all of the adults in the traps at Place 7 and Place 8 were
1041 collected, while 20 out of 37 were collected at Place 9. (B, D, and F) The relative abundances of
1042 fungi or bacteria in the fermented banana or fly samples. The compositions were analyzed using
1043 primer sets amplifying the fungal ITS region or bacterial 16S rDNA region. Operational taxonomic
1044 units (OTUs) accounting for >1% were grouped by families, as shown. The ratio of those
1045 accounting for <1% was summed and is indicated as "Others." The genera belonging to uncertain
1046 families (incertae sedis) are indicated by their genus name in parentheses. (B) The result
1047 corresponding to the sampling depicted in (A). The numbers on the horizontal axis indicate each
1048 numbered sampling location. (D and F) The result corresponding to the sampling depicted in (C)
1049 and (E), respectively. E, early-stage food; L, late-stage food; Susp, microbial suspension; w/o L,
1050 late-stage food without larvae; w/ L, late-stage food with larvae; Lar, larvae.

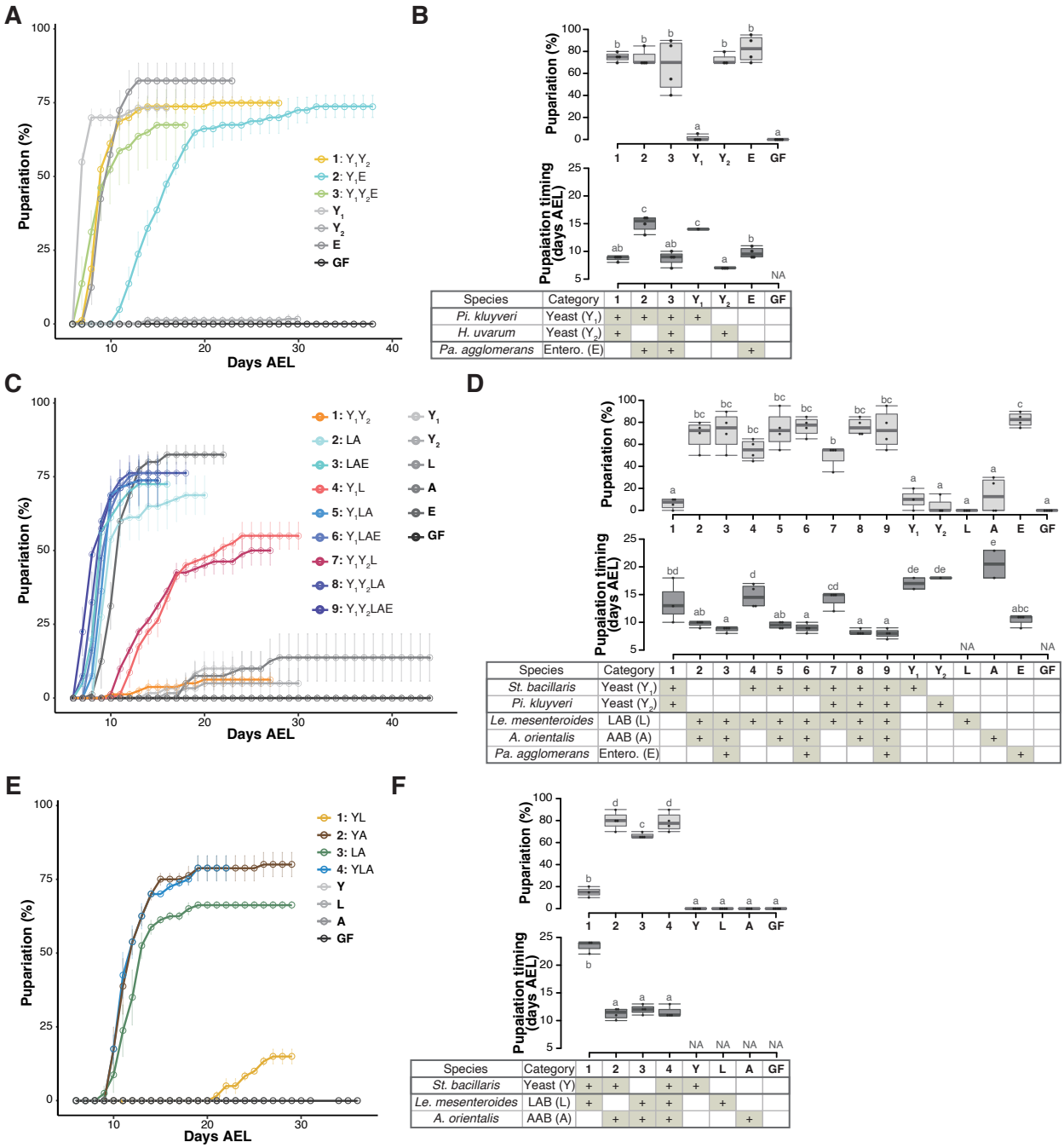

1051 Figure 2. Mure et al.

1052 **Figure 2. Prominent acceleration of larval development occurred with early-stage-dominant**
1053 **yeast alone, as well as in combination with late-stage-dominant acetic acid bacteria and other**
1054 **microbes**

1055 (A-F) The percentage and timing of pupariation of larvae feeding on microbes detected in the
1056 early-stage food (A and B), or five (C and D) or three (E and F) microbes detected in the late-stage
1057 food from Sampling Place 1 in Figure 1B. (A, C, and E) Each data point represents the average
1058 percentage of individuals per tube that pupariated by each day. n=3-4. Colored lines are for mixed
1059 conditions, while gray lines are for mono-associated or germ-free conditions. The codes for
1060 individual species are provided in the chart at the bottom of (B), (D), and (E), respectively. (C)
1061 The color coding for the respective foods is as follows: includes yeasts only (orange); includes
1062 yeast(s) and LAB but no AAB (red); includes LAB and AAB (blue). (B, D, and F) Percentage of
1063 the larvae pupariated (pupariation ratio; upper) and the timing at which 50% of the pupariation
1064 ratio was achieved (lower). Boxes represent upper and lower quartiles, while the central lines
1065 indicate the median. Whiskers extend to the most extreme data points, which are no more than 1.5
1066 times the interquartile range. Unique letters indicate significant differences between groups
1067 (Tukey-Kramer test, $p < 0.05$). GF, germ-free; days AEL, days after egg laying.

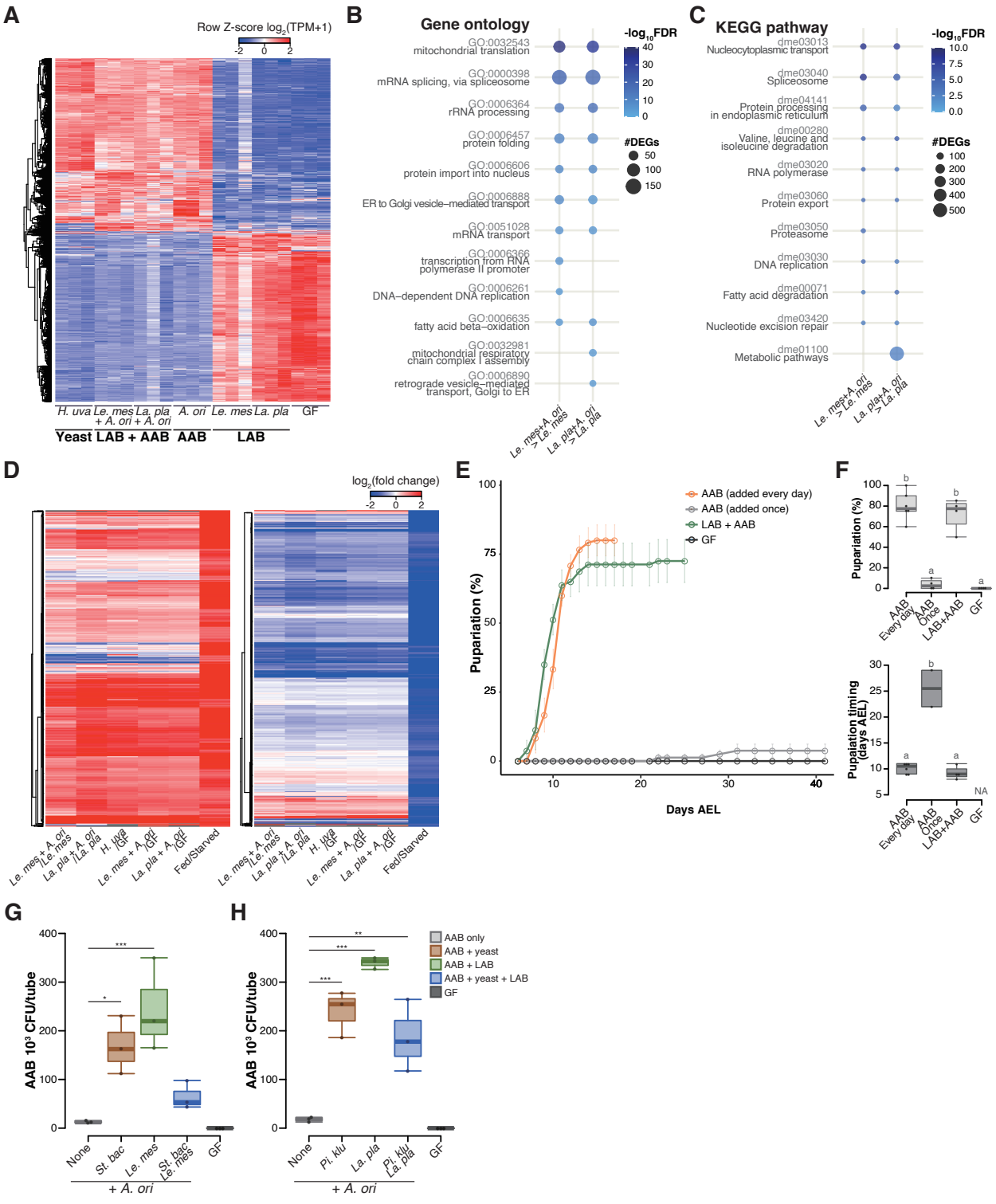

1068 Figure 3. Mure et al.

Figure 3. During the late stage, acetic acid bacteria play a crucial role in supporting larval development through interspecies interactions among the microbes

(A) Heat map of gene expression values for first instar larvae fed *H. uvarum* or bacteria. Freshly hatched germ-free larvae were placed on banana agar inoculated with each microbe and collected after 15 h feeding to examine gene expression of the whole body. (B and C) Plots showing the result of GO term (B) or KEGG Pathway (C) enrichment analysis of the RNA-seq data. 10 terms/pathways that showed the smallest FDR in each analysis are shown. (D and E) Heat maps showing the similarity between our RNA-seq data and microarray data in a previous study (Zinke et al., 2002). Zinke et al. used larvae at 47-49 h AEL and fed them yeast paste or starved them for 12h before comparing the gene expression profiles. The data from Zinke et al., 2002. are labeled as "Fed/Starved" in the righthand column of each heat map. Only the genes exhibiting more than 2-fold changes in their analysis are shown. Our data were calculated using TPM of each gene in the larvae on the supportive conditions versus those on the non-supportive conditions. (E and F) The percentage and timing of pupariation of the larvae feeding on AAB on banana agar. Graphs are presented as in Figure 2. n=3-4. (G and H) AAB load of foods inoculated with AAB, with or without other microbial species. Boxplots are depicted as in Figure 2 (Dunnett's test, $*p < 0.05$, $**p < 0.01$, $***p < 0.001$). *La. pla*, *Lactiplantibacillus plantarum*; *Le. mes*, *Leuconostoc mesenteroides*; *A. ori*, *Acetobacter orientalis*; *H. uva*, *Hanseniaspora uvarum*; *St. bac, Starmerella bacillaris*; *Pi. klu*, *Pichia kluyveri*; GF, germ-free; days AEL, days after egg laying.

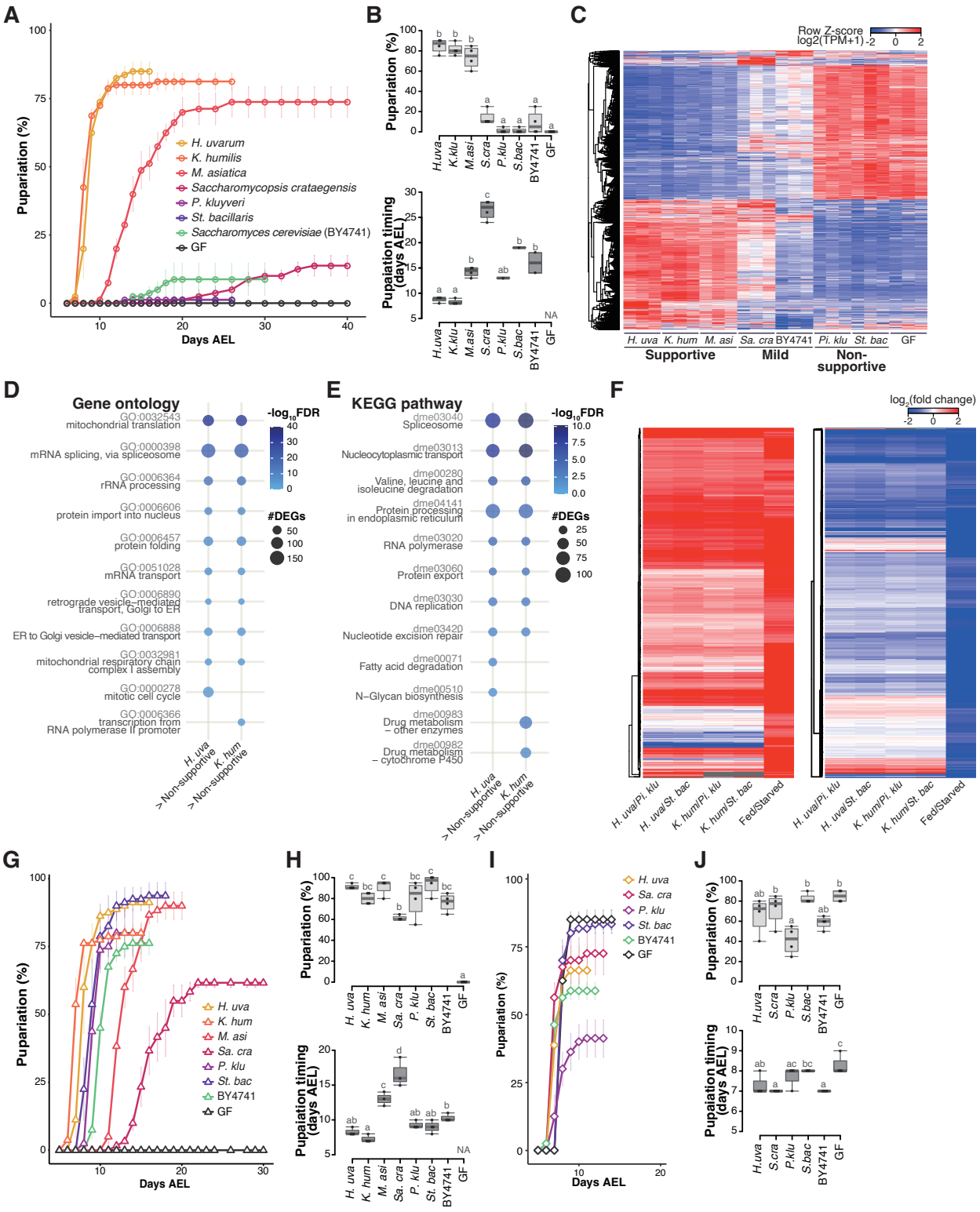

Figure 4. Mure et al.

1089 **Figure 4. Isolated yeast species promote larval development to varying degrees, but all**
1090 **support larval development upon heat killing**

1091 (A and B) The percentage and timing of pupariation of larvae feeding on live yeasts on banana
1092 agar. Graphs are presented as in Figure 2. n= 3-4. (C) Heat map of gene expression values for first
1093 instar larvae fed on each yeast species. Freshly hatched germ-free larvae were placed on banana
1094 agar inoculated with each microbe and collected after 15 h feeding to examine gene expression of
1095 the whole body. (D and E) Plots showing the result of GO term (D) or KEGG Pathway (E)
1096 enrichment analysis of the RNA-seq data. Genes that showed significantly higher expression on
1097 each of the supportive species than on both the non-supportive species were analyzed. 10
1098 terms/pathways that showed the smallest FDR in each analysis are shown. (F) Heat maps showing
1099 the similarity between our RNA-seq data and microarray data in Zinke et al., 2002, shown as
1100 described in Figure 3. (G-J) The percentage and timing of pupariation of the larvae feeding on
1101 heat-killed yeasts on banana agar (H and I) or live yeasts on a nutritionally rich medium (J and K).
1102 Graphs are depicted as in Figure 2. n=3-4. *H. uva*, *Hanseniaspora uvarum*; *K. hum*, *Kazachstania*
1103 *humilis*; *M. asi*, *Martiniozyma asiatica*; *Sa. cra*, *Saccharomycopsis crataegensis*; *Pi. klu*, *Pichia*
1104 *kluyveri*; *St. bac*, *Starmerella bacillaris*; GF, germ-free; days AEL, days after egg laying.

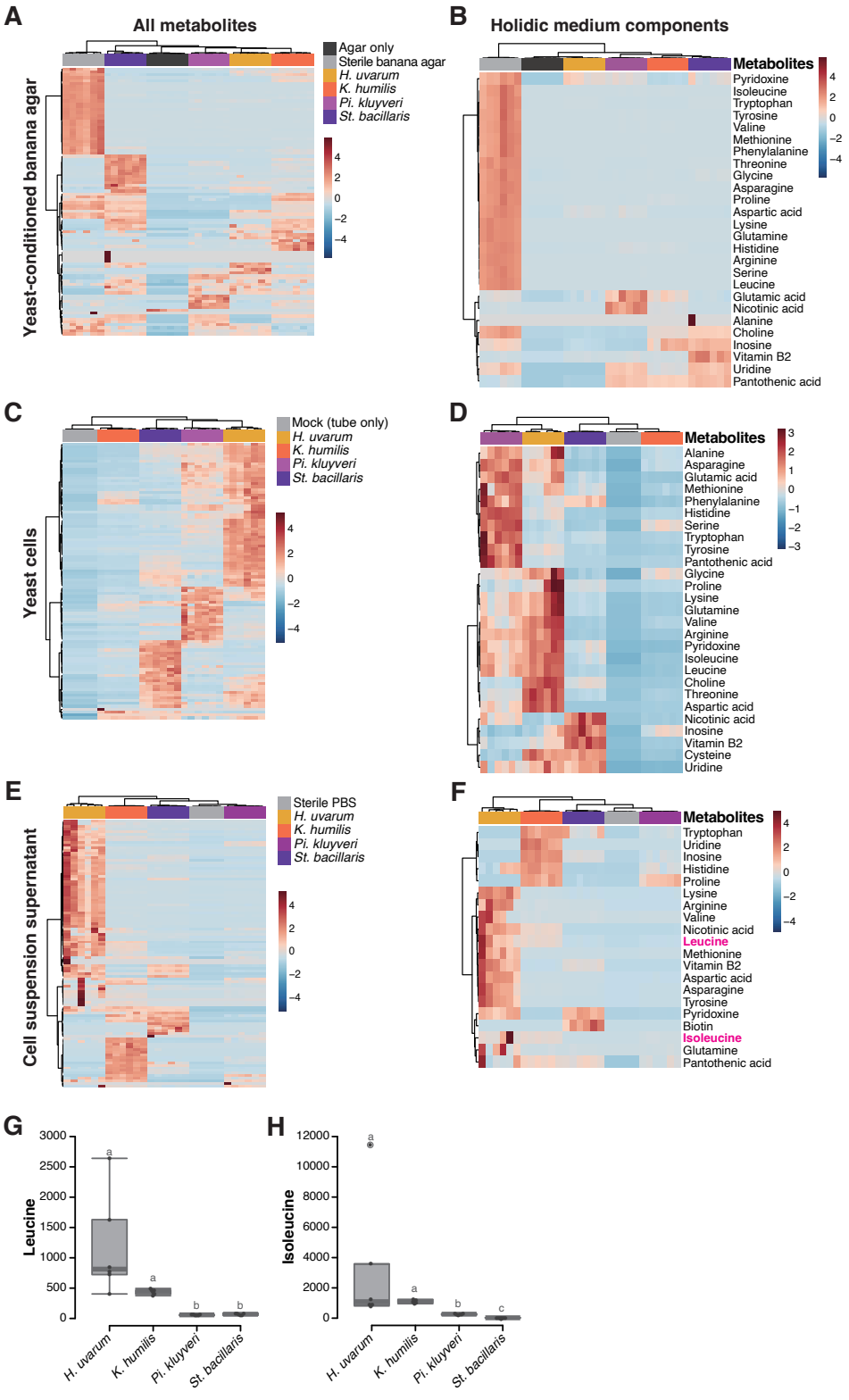

1105 Figure 5. Mure et al.

1106 **Figure 5. Metabolomic analysis of yeast cells, yeast-conditioned banana-agar plates, or cell**
1107 **suspension supernatants**

1108 (A-F) Heat maps showing all detected metabolites (A, C, and E) or only the metabolites included
1109 in a chemically defined synthetic (holidic) medium for *Drosophila melanogaster* (Piper et al.,
1110 2014) (B, D, and F) detected from the metabolomic analysis of banana-agar plates (A and B), yeast
1111 cells (C and D), or yeast-cell suspension supernatants (E and F). (G and H) Normalized peak areas
1112 of leucine (G) and isoleucine (H) in yeast-cell suspension supernatants. Boxplots are presented as
1113 in Figure 2.

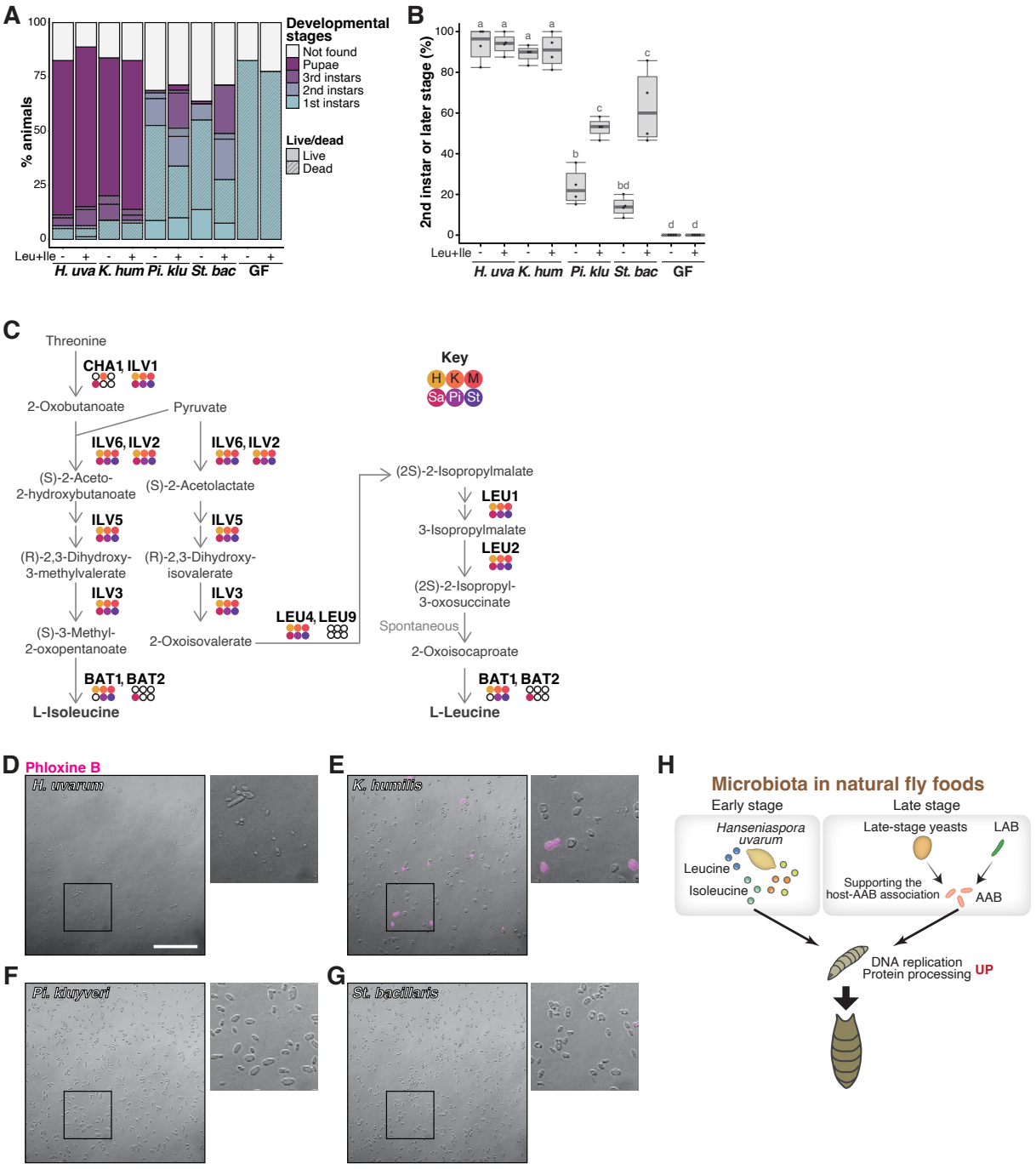

Figure 6. Mure et al.

1115 **Figure 6. Supportive yeasts facilitate larval growth by providing nutrients, including**
1116 **branched-chain amino acids, by releasing them from their cells**

1117 (A and B) Growth of larvae feeding on yeasts on banana agar supplemented with leucine and
1118 isoleucine. (A) The mean percentage of the live/dead individuals in each developmental stage. n=4.
1119 (B) The percentage of larvae that developed into second instar or later stages. The "Not found"
1120 population in Figure 6A was omitted from the calculation. Each data point represents data from a
1121 single tube. Unique letters indicate significant differences between groups (Tukey-Kramer test, p
1122 < 0.05). (C) The biosynthetic pathways for leucine and isoleucine with *S. cerevisiae* gene names
1123 are shown. The colored dots indicate enzymes that are conserved in the six isolated species, while
1124 the white dots indicate those that are not conserved. Abbreviations of genera are given in the key
1125 in the upper right corner. LEU2 is deleted in BY4741. (D-G) Representative image of Phloxine B-
1126 stained yeasts. The right-side images are expanded images of the boxed areas. The scale bar
1127 represents 50 μm. (H) Summary of this study. *H. uvarum* is predominant in the early-stage food
1128 and provides Leu, Ile, and other nutrients that are required for larval growth. In the late-stage food,
1129 AAB directly provides nutrients, while LAB and yeasts indirectly contribute to larval growth by
1130 enabling the stable larva-AAB association. The host larva responds to the nutritional environment
1131 by dramatically altering gene expression profiles, which leads to growth and pupariation. *H. uva*,
1132 *Hanseniaspora uvarum*; *K. hum*, *Kazachstania humilis*; *Pi. klu*, *Pichia kluyveri*; *St. bac*,
1133 *Starmerella bacillaris*; GF, germ-free.

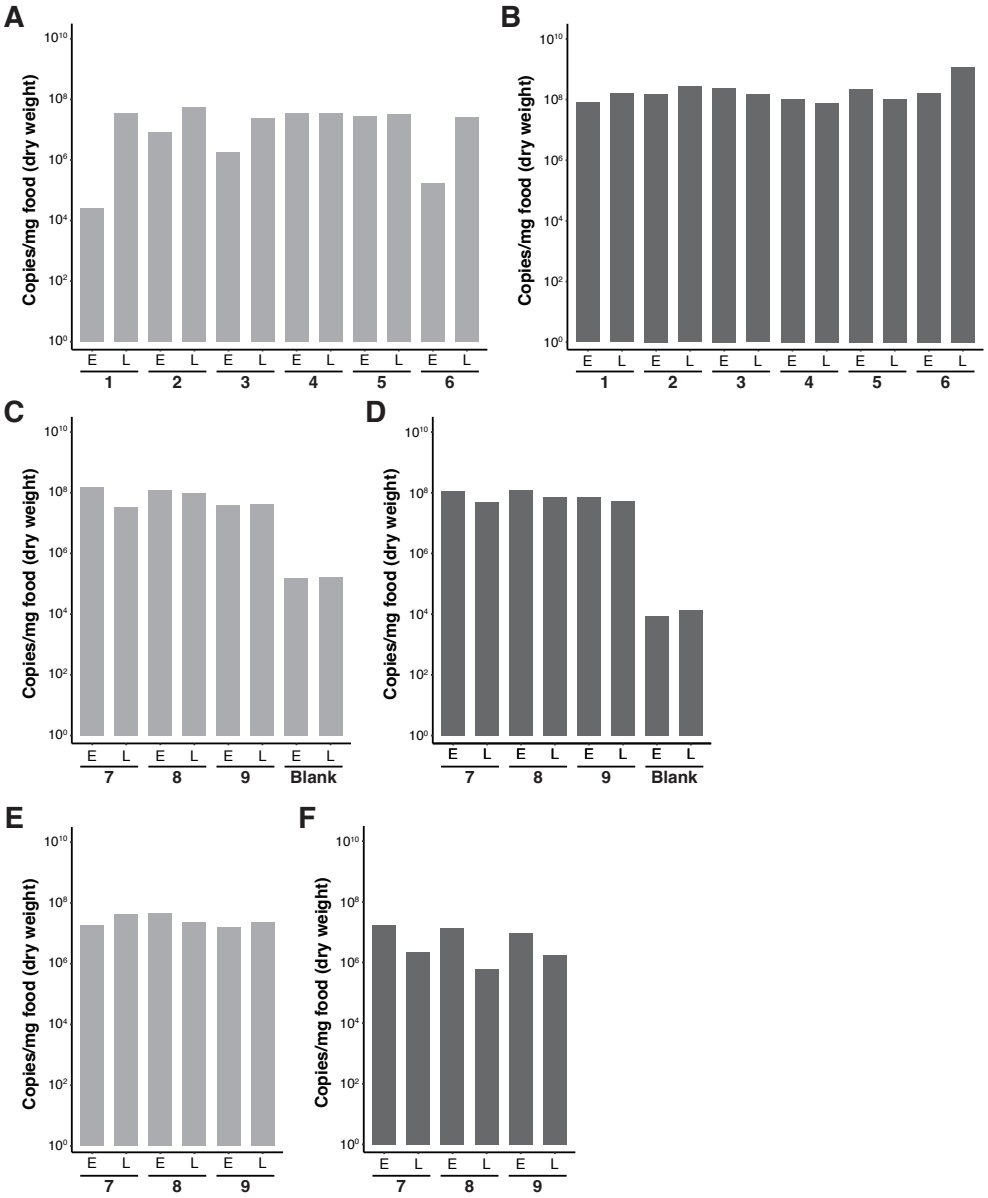

1134 Figure S1. Mure et al.

1135 **Figure S1. Copy numbers of microbial rDNA in fermented banana samples.**

1136 (A-F) Graphs showing the copy numbers of the fungal ITS region (A, C, and E) or bacterial 16S
1137 rRNA region (B, D, and F) in the fermented food samples shown in Figures 1A and 1B (A and B),
1138 Figures 1C and 1D (C and D), and Figures 1E and 1F (E and F). Numbers below each pair of foods
1139 indicate the sampling places, which correspond to those indicated in Figure 1. (C and D) Yeast
1140 and bacteria were also detected in Blank samples, in which sterile PBS instead of microbial
1141 suspensions was added. They might have invaded the fruit by passing through wounds on the peel
1142 (Oyewole, 2012). E: early-stage food; L: late-stage food.

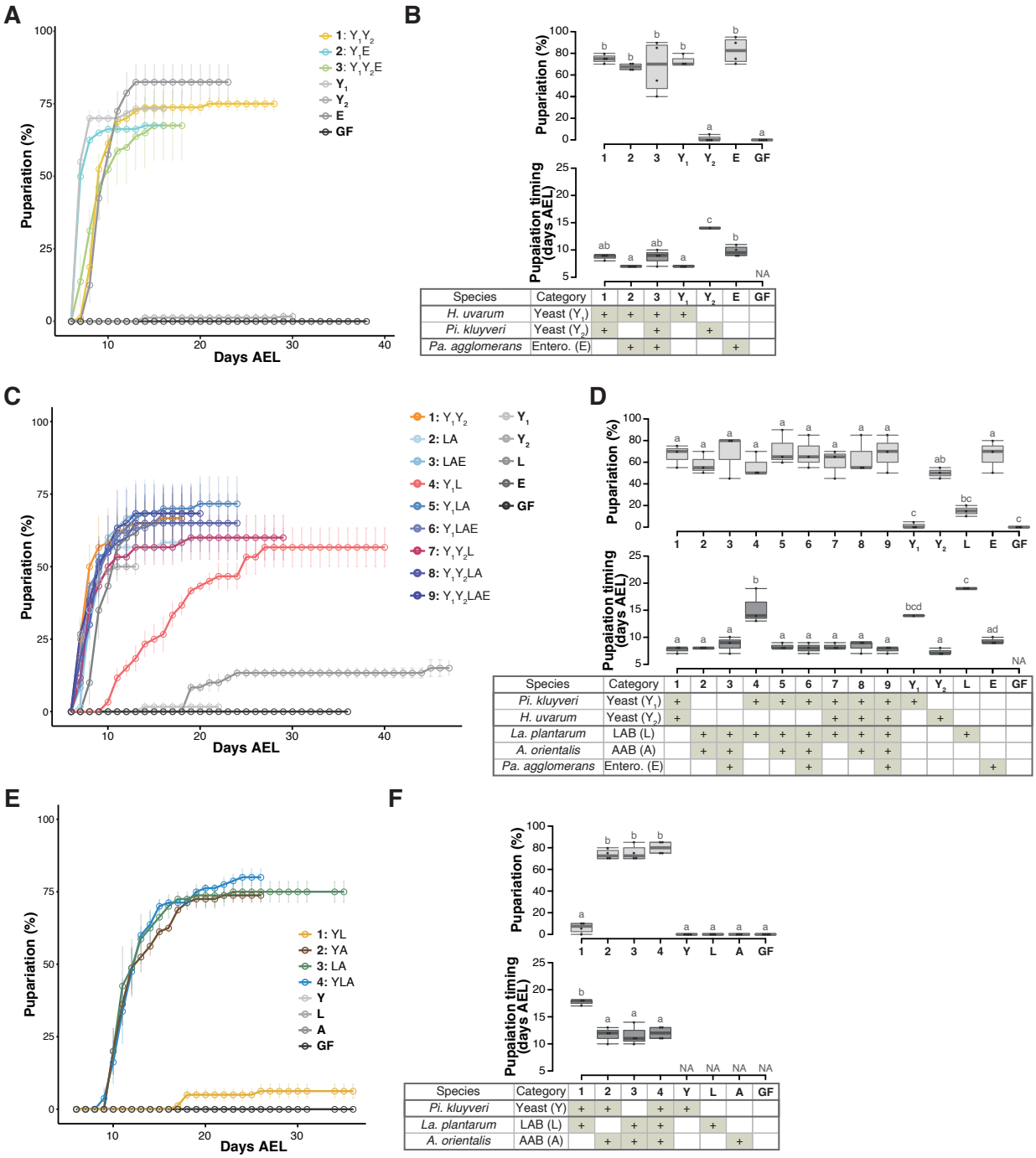

1143 Figure S2. Mure et al.

1144 **Figure S2. Larvae feeding on mixtures of isolated microbial species detected in the samples**
1145 **from Sampling Place 2 in Figure 1B.**

1146 (A-F) The percentage and timing of pupariation of larvae feeding on (A and B) microbes derived
1147 from the early-stage food, or (C and D) five, or (E and F) three microbes derived from the late-
1148 stage food. (A, C, and E) The codes for individual species are provided in the chart at the bottom
1149 of (B), (D), and (F), respectively. (B, D, and F) Graphs are presented as in Figure 2. n=3-4. GF,
1150 germ-free; days AEL, days after egg laying.

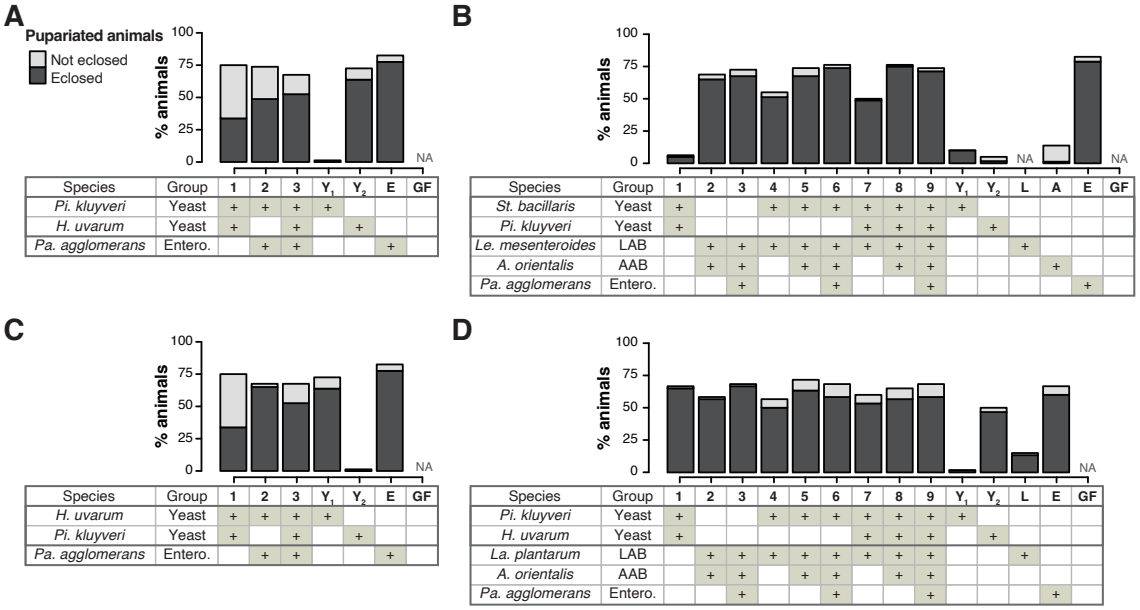

1151 Figure S3. Mure et al.

1152 **Figure S3. The percentage of pupariation and eclosion of the larvae feeding on microbes.**

1153 (A-D) Graphs showing the percentage of larvae that pupariated in the experiments shown in
1154 Figures 2A and 2B (A), Figures 2C and 2D (B), Figures S2A and S2B (C), or Figures S2C and
1155 S2D (D). The mean percentages of the pupariated and eclosed (dark gray) or pupariated and not
1156 eclosed (light gray) individuals are shown. n=3-4.

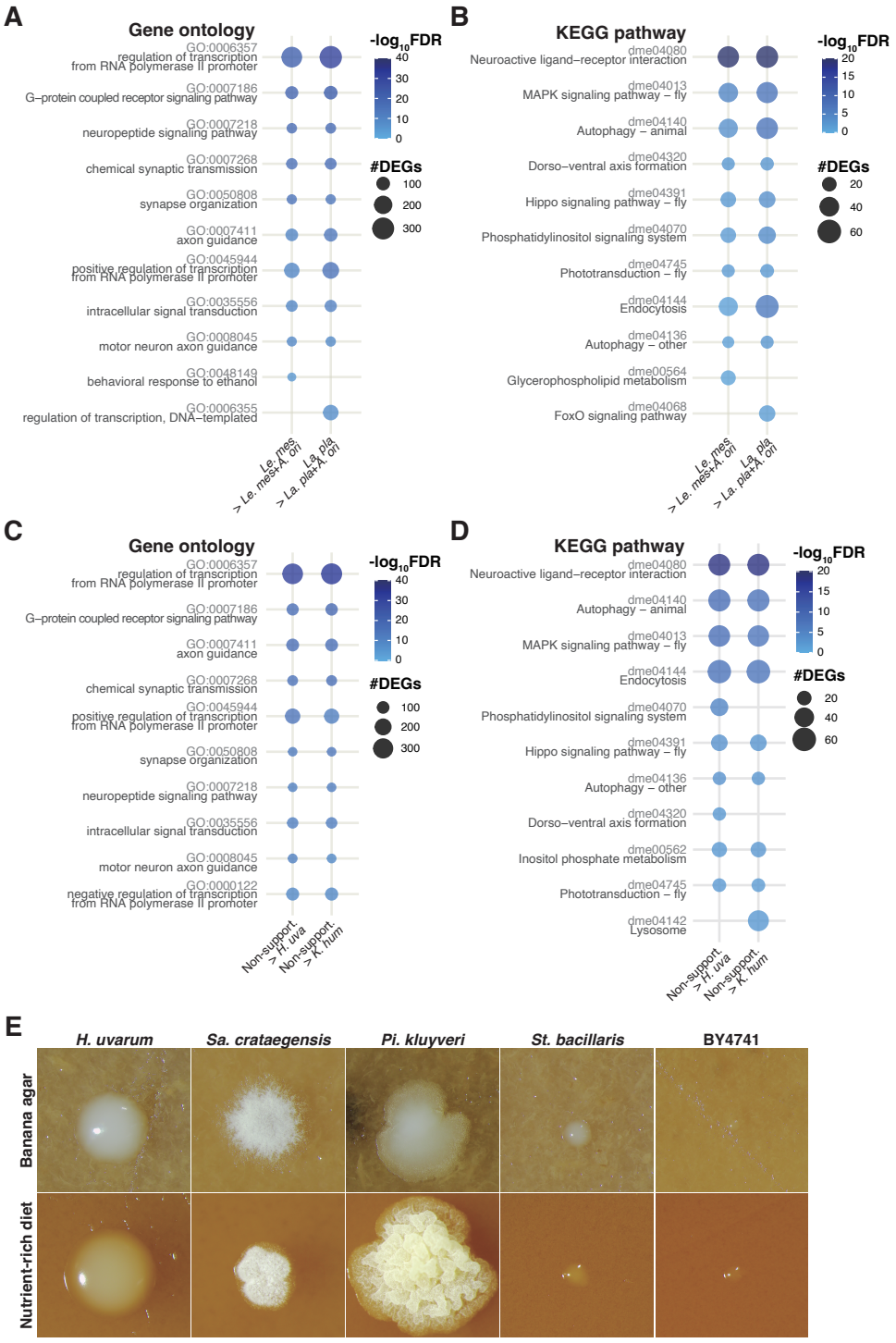

1157 Figure S4. Mure et al.

1158 **Figure S4. Enrichment analyses of the genes upregulated in non-supportive conditions and**
1159 **morphology of yeast colonies grown on a nutrient-rich diet.**
1160 (A–D) Plots showing the result of GO term (A and C) or KEGG Pathway (B and D)
1161 enrichment analysis of the RNA-seq data shown in Figure 3A (A and B) and Figure 4C (C and
1162 D). Plots were generated as described in Figure 3. (E) Images of single yeast colonies grown
1163 on banana agar or the nutrient-rich diet. The images were taken after a 2-day incubation at
1164 25° C.

Table 1. List of microbial species used in the feeding experiments.

Percentages indicate the relative abundance of each species in the foods shown in Figure 1B.

Yeast or bacterium	Fermentation stage	Family	Species	Sampling place 1 (early stage)	Sampling place 1 (late stage)	Sampling place 2 (early stage)	Sampling place 2 (late stage)
Yeast	Early	Saccharomycodaceae	*Hanseniaspora uvarum*	20.93%		79.28%	2.11%
Yeast	Late	Pichiaceae	*Pichia kluyveri*	40.09%	26.26%	19.07%	97.14%
Yeast	Late	incertae sedis	*Starmerella bacillaris*		72.97%		
Bacterium	Early	Erwiniaceae	*Pantoea agglomerans*	45.31%	12.81%	90.56%	6.17%
Bacterium	Late	Lactobacillaceae	*Leuconostoc mesenteroides*		54.17%		
Bacterium	Late	Lactobacillaceae	*Lactiplantibacillus plantarum*				60.84%
Bacterium	Late	Acetobacteraceae	*Acetobacter orientalis*		8.25%		15.48%

1167 **Supplementary Files**

1168 Table S1. List of adult flies caught in the traps.

1169

1170 Table S2. Microbial composition analysis results.

1171

1172 Table S3. Microbial isolation and species identification.

1173

1174 Table S4. Table S3. RNA-seq data of whole bodies of 1st instar larvae fed on *H. uvarum* or bacteria.

1175

1176 Table S5. RNA-seq data of whole bodies of 1st instar larvae fed on yeasts

1177

1178 Table S6. Results of metabolomic analysis of yeast samples.

1179

1180 Table S7. Final genome assembly and annotation statuses of six yeast strains.

1181

1182 Table S8. RNA-seq data of isolated yeasts.

1183

1184 Table S9. Statistical details of experiments.